NASA TECHNICAL NOTE

NASA TN D-7055

NASA TN D-7055

EFFECTIVE THERMAL CONDUCTIVITIES OF FOUR METAL-CERAMIC COMPOSITE COATINGS IN HYDROGEN-OXYGEN ROCKET FIRINGS

by Ralph L. Schacht, Harold G. Price, Jr., and Richard J. Quentmeyer

Lewis Research Center
Cleveland, Ohio 44135

NATIONAL AERONAUTICS AND SPACE ADMINISTRATION • WASHINGTON, D. C. • NOVEMBER 1972

1. Report No.	2. Government Accession No.	3. Recipient's Catalog No.
TN D-7055		

4. Title and Subtitle	5. Report Date
EFFECTIVE THERMAL CONDUCTIVITIES OF FOUR METAL-CERAMIC COMPOSITE COATINGS IN HYDROGEN-OXYGEN ROCKET FIRINGS	November 1972
	6. Performing Organization Code
7. Author(s)	8. Performing Organization Report No.
Ralph L. Schacht, Harold G. Price, Jr., and Richard J. Quentmeyer	E-7035
9. Performing Organization Name and Address	10. Work Unit No.
Lewis Research Center National Aeronautics and Space Administration Cleveland, Ohio 44135	503-35
	11. Contract or Grant No.
12. Sponsoring Agency Name and Address	13. Type of Report and Period Covered
National Aeronautics and Space Administration Washington, D.C. 20546	Technical Note
	14. Sponsoring Agency Code

15. Supplementary Notes

16. Abstract

An experimental investigation was conducted at the NASA Lewis Research Center to determine the effective conductivities of four plasma-arc-sprayed, metal-ceramic gradated coatings on hydrogen-oxygen thrust chambers. The effective thermal conductivities were not a function of pressure or oxidant-to-fuel ratio. The various materials that made up these composites do not seem to affect the thermal conductivity values as much as the differences in the thermal conductivities of the parent materials would lead one to expect. Contact resistance evolving from the spraying process seems to be the controlling factor. The thermal conductivities of all the composites tested fell in the range of 0.75 to 7.5 watts per meter kelvin (0.1×10^{-4} to 1.0×10^{-4} Btu/(sec)(in.)(^{o}R)).

17. Key Words (Suggested by Author(s))

Heat transfer
Metal and ceramic rocket coatings
Hydrogen-oxygen rocket engines

18. Distribution Statement

Unclassified - unlimited

19. Security Classif. (of this report)	20. Security Classif. (of this page)	21. No. of Pages	22. Price*
Unclassified	Unclassified	42	$3.00

* For sale by the National Technical Information Service, Springfield, Virginia 22151

EFFECTIVE THERMAL CONDUCTIVITIES OF FOUR METAL-CERAMIC COMPOSITE COATINGS IN HYDROGEN-OXYGEN ROCKET FIRINGS

by Ralph L. Schacht, Harold G. Price, Jr., and Richard J. Quentmeyer

Lewis Research Center

SUMMARY

An experimental investigation was conducted at the NASA Lewis Research Center to determine the effective thermal conductivities of four plasma-arc-sprayed, metal-ceramic gradated coatings on hydrogen-oxygen thrust chambers. Within the accuracy and range of the tests, the effective thermal conductivities of the composite coatings were not a function of pressure and oxidant-to-fuel ratio. The rockets were operated over a range of pressures from 2.068 to 6.205×10^{6} newtons per square meter (300 to 900 psia) and over a range of oxidant-to-fuel ratios from 3 to 7.33. The effective conductivities of the composites tested all fell in the range of approximately 0.75 to 7.5 watts per meter kelvin (0.1×10^{-4} to 1×10^{-4} Btu/(sec)(in.)(^{o}R)), with the bulk of the data at about 3 watts per meter kelvin (0.4×10^{-4} Btu/(sec)(in.)(^{o}R)). The various materials that made up these composites do not seem to affect the effective thermal conductivity values as much as the differences in the thermal conductivities of the parent materials would lead one to expect. Contact resistance evolving from the spraying process seems to be the controlling factor. The effective thermal conductivities of the coatings are such that they can be used to provide very effective thermal barriers.

INTRODUCTION

Coatings have been used for heat barriers for many years in various applications. Their use in rocket nozzles has been greatly curtailed because the coatings are continually plagued with cracking and spalling problems. One of the factors that cause this cracking and spalling is thermal stress caused by the high temperature differential that exists across the coating. Plasma-arc-sprayed, gradated coatings, where a gradual transition is made from a metal to a ceramic, should be a means of controlling temperature differentials, because of the differences in the conductivities. Gradated properties

should reduce and distribute across the thickness the thermal stresses which would otherwise concentrate at the metal/ceramic interface, where the gross change in properties occurs. Therefore, to control the temperature differential across the various layers, the effective conductivities must be known. The conductivities of the bulk materials that make up the coating are fairly well known, but the as-sprayed effective conductivities are unknown, especially in the environment of high pressure and temperature encountered in a rocket nozzle.

R. P. Tye carried out an investigation (unpublished work done at Dynatech Corporation under contract NAS 3-11632) on a number of composites in a vacuum of 0.133 to 0.0133 newtons per square meter (10^{-3} to 10^{-4} torr) and at operating temperatures of 533 and 1363 K (959° and 2453° R). He found great variations of the conductivities with temperature and two orders of magnitude variations in conductivity for the same composites made by different vendors. Aerojet General (ref. 1) also developed a thermal-barrier coating which was used on a water-cooled nozzle and fired with a solid-propellant rocket motor. Conductivities for this coating were determined by cycling specimens in and out of a plasma flame and also from thermal diffusivity measurements, but again, the results of reference 1 differed from those of Tye and were not obtained under actual rocket conditions.

The investigators of references 2 and 3 made up disk coupons to obtain thermal resistances for a group of coatings. A plasma torch under controlled heat flux was again used for these tests. The thermal conductivities obtained from these data were considered qualitative because of possible inaccuracies in measuring heat flux and surface temperature. The results of this method were compared with those of the thermal flash method. The data agreed within about 20 percent. These reports make a general statement that the thermal conductivities were generally 40 percent of handbook values. Melting occurred in all of the coatings containing metal additions and appeared to increase with increased metal content. The regression rates were excessive for molybdenum-ceramic mixtures containing molybdenum additions above 27 weight percent. No mention of contact resistance affecting the conductivities is made in references 1 to 3.

Boganov et al. (ref. 4) found that ceramic coatings produced by the method of oxy-aceteylene flame spraying have very low effective thermal conductivities. Reference 4 used coatings of aluminum oxide, zirconium dioxide, titanium dioxide, zircon, and spinel ($MgO\ Al_2O_3$). Measurements were carried out in a vacuum of 1.333×10^{-3} newtons per square meter (10^{-5} mm Hg) and in an argon atmosphere at pressures of 1.333×10^4 and 3.999×10^4 newtons per square meter (100 and 300 mm Hg), in the temperature range of 573 to 1173 K (1031° to 2111° R). The values of thermal conductivity increased with increasing pressure of the argon and with increasing temperature. The effective conductivities of the coatings were all of the same order of magnitude despite

the considerably different thermal conductivities of the materials themselves. The values of the effective thermal conductivities were, on the average, less by factors of 5 to 10 than the values usually given for the same materials calculated in the form of monolithic specimens with porosities of 20 to 30 percent. Two factors were used to explain the findings of reference 4: small effective area of direct contact between coating and base and between individual particles, and blocks of particles in the arbitrary layers of the coating.

Curren et al. (ref. 5) also ran tests in a plasma flame for a group of composites. Some of these composites looked good for rocket applications, but the values of conductivity and the behavior characteristics of the composites in a rocket combustion environment remained unknown.

Since the conductivity of a sprayed porous ceramic may be affected by the mixture ratio, pressure, and temperature of the gas entrained from the boundary layer of a rocket thrust chamber, it is essential that the conductivity data be obtained in that environment. It was also necessary to resolve some of the contradictory findings of references 1 to 5. In order to attack these problems, an experimental investigation was conducted at the Lewis Research Center with the use of heat-sink copper thrust chambers, with sectors of these thrust chambers coated with the various layers that make up the composite coatings. The hydrogen-oxygen rocket was then fired, and with the transient-temperature technique developed in reference 6, the effective heat-transfer coefficients obtained from the various sectors were compared with those obtained from an uncoated sector or with the heat-transfer coefficients that these sectors had before coating. Values of the effective thermal conductivity were determined from these measurements for both the individual layers and the complete composites under actual rocket operating conditions.

Two copper thrust chambers were used. Hereinafter, these thrust chambers will be designated Cu II and Cu III. (Thrust chamber Cu I was used in the work of ref. 6.) Thrust chamber Cu II had six 60° sectors that ran axially through its entire length. One of these 60° sectors was always left uncoated. The other sectors were coated with one or more of the layers that made up the complete composite, with at least one of the sectors coated with the complete composite. This allowed tests of composites made up of as many as five layers. Thrust chamber Cu III had two sectors that ran axially throughout the entire length. One sector of 60° was left uncoated, and the other 300° sector was always coated with the total number of layers that made up the composite.

Thrust chamber Cu II could thus give details on the various layers, while thrust chamber Cu III was used to check the repeatability of the coating application and to give a better statistical evaluation of the effective conductivity for the complete composite.

For the four composite coatings tested, the thrust chambers were operated over a range of pressures from 2.068×10^{6} to 6.20×10^{6} newtons per square meter absolute (300

to 900 psia) and over a range of oxidant-to-fuel ratios from 3 to 7.33 (hydrogen fuel from 25 to 12 percent by weight).

APPARATUS AND EXPERIMENTAL PROCEDURE

Thrust-Chamber Design

Two copper heat-sink, solid-wall, hydrogen-oxygen thrust chambers were used in the experiments to obtain transient temperature data. The geometries of the two thrust chambers (Cu II and Cu III) were identical and were the same as those used in references 6 and 7. The contraction and expansion area ratios were 4.64. The contraction half angle was 30°, and the expansion half angle was 15°. The length of the combustion chamber from the injector to the throat was 0.3683 meter (14.5 in.). The characteristic length L^* was 1.372 meters (54 in.). The throat diameter was 0.127 meter (5 in.). The rocket developed 1.15×10^5 newtons (26 000 lb) of thrust at a chamber pressure of 6.205×10^6 newtons per square meter absolute (900 psia).

Thrust chamber Cu II (fig. 1) was always coated with the various coating layers on five sectors (approx. 60° each) that extended axially through the entire length, with one 60° sector left uncoated. Thrust chamber Cu III (fig. 2) always had one 60° sector uncoated and the other 300° sector coated with the complete composite of all layers. Thrust chamber Cu II thus had the capability of determining the conductivity of the first layer, the first two layers, etc., up to a maximum of five layers of a composite coating system. Thrust chamber Cu III had 10 axial measuring stations compared to five for Cu II and was used to see how repeatable the coating systems were and also to give more data so that statistically the conductivity of the complete composite systems could be more accurately determined.

Thin copper shields were used in the thrust chamber to protect the other sectors as the various layers of the composite were plasma sprayed onto the thrust chamber. These shields were then cut at the various axial instrumentation stations and were polished. Photomicrographs were then made at a magnification of 250, and the thicknesses of the coatings on the various sectors were measured. Previous photomicrographic work was used to make sure that the compositions were right. A typical set of photomicrographs is shown in figure 3 for composite coating type 3. Ten readings of thickness were taken per photomicrograph and then were averaged.

Dummy plugs were also added at the chamber and throat axial stations. These plugs were to be removed after running to check thicknesses and chemical compositions of the coatings. Unfortunately, these plugs were not designed with the same threaded mechanism as were the instrumented plugs. The movement of these dummy plugs

caused the coating to pop off immediately during running.

A coaxial injector (fig. 4) was used with liquid oxygen and gaseous hydrogen as the propellants. This injector was the same as those used in references 6 and 7. The injector had 234 injector elements uniformly spaced in a disk-shaped faceplate (2.6 elements per square inch). Because previous running had indicated a possible hot region near the injector face (ref. 7), 72 peripheral cooling holes were added as an outer ring on the injector face. The diameter of these holes was 0.6601×10^{-3} meter (0.026 in.). They were located so that the jets of hydrogen hit the thrust-chamber wall approximately 0.0254 meter (1 in.) downstream of the injector face. The coolant flow through these holes was approximately 1.5 percent of the hydrogen propellant flow at an operating chamber pressure of 2.068×10^{6} newtons per square meter absolute (300 psia) and an oxidant-to-fuel ratio of 5.67 (15 percent fuel).

Composite Coatings

Curren et al. (ref. 5) of the Lewis Research Center studied a number of composite coatings made up of as many as five layers. These layers were made up of various materials to make a gradual transition from a metal surface to a ceramic surface. The transition was made to obtain coatings that would survive in the operating regimes of a rocket engine. Four of these coating composites seemed promising and, therefore, were chosen for study in this experiment. Tables I and II give the details of these composites, including the design thickness and the measured thickness.

Figure 5 shows the spray rig used to apply the coatings to the rocket thrust chambers. The coatings were applied with a Plasmadyne SG-3, 25-kilowatt, 5.08-centimeter (2-in.) gun. The spray angle of the gun was kept perpendicular and at a constant distance of 5.08 centimeters (2 in.) from the surface in the chamber and throat regions. The spray coating rig, however, did not have enough flexibility to maintain this optimum angle and constant distance in the exit cone. The angle was kept perpendicular to the nozzle axis and the distance from the surface increased as the exit cone was traversed. Even in the chamber and throat regions the design thicknesses were not always achieved, as is shown by tables I and II. Because photomicrographs were obtained that gave the coating thicknesses, it was not considered essential to spend the time, money, and effort needed to develop the sophisticated system needed to apply a very uniform and prescribed thickness of coating to a thrust chamber with a 0.127-meter (5-in.) throat diameter. Photomicrographs of two areas circumferentially 180° apart but at the same axial station showed a maximum variation of 28 percent in thickness for the coating on one of the thrust chambers. The photomicrographic thicknesses were used in all calculations. After the test of a coating was completed, the coating was removed, and the nozzle was

recoated with another composite type. Composite-coating types 2 and 3 were made up of five layers. Layered coating type 5 had three layers, and composite coating type 6 had two layers.

Instrumentation and Data Recording

Rods of pure oxygen-free copper, 0.00572 meter (0.225 in.) in diameter, inserted in holes machined normal to the inside wall of the thrust chamber, were used to approximate a one-dimensional, semi-infinite slab. Four Chromel-Alumel thermocouples were used on each rod to obtain the transient temperature data. The geometry, construction, installation, sealing, and pressurizing details of these rods are the same as those used in reference 6. Table III gives a summary of the angular and axial locations of the rods for both thrust chambers. These locations are the same as those in reference 7. Table III lists 12 axial stations for Cu III, but only 10 gave effective heat-transfer coefficients.

Propellant flow, chamber pressure, and rod temperatures were recorded in a digitized form on a magnetic tape for direct entry into a digital computer. These same data were stored in the IBM 360 time-sharing system, with direct access from a terminal in the control room. This allowed the main output results to be reviewed between runs and allowed the program to be monitored and modified on the spot by using these results. The digitizing system had a sampling rate of 25 000 words per second, and 100 parameters were sampled. Data parameters were fitted over a 25-word sampling interval with smoothing to eliminate 60-hertz noise and greatly diminish any random noise.

The calculating procedure fit a smooth curve through 25 readings of the data parameter. Then, one report was made for all parameters at a common time, and terminal calculations were carried out as many times as desired. This reduced the amount of terminal calculations. Chamber pressure, which was sampled many times in the 100-word block, was used as a triggering device for starting and stopping calculations for the transient tests.

Test Procedure

The rocket engine (fig. 6) was installed on a test stand located at the Lewis Research Center. Propellant valves for controlling gaseous hydrogen and liquid oxygen were prepositioned before the run and were opened to these fixed positions during the run to provide the desired values for chamber pressure and mixture ratio. Chamber pressures were varied from 2.068×10^6 to 6.205×10^6 newtons per square meter absolute (300 to 900 psia) at oxidant-to-fuel ratios of 3.0 to 7.33 (hydrogen fuel from 25 to

12 percent). The timing and sequencing of the valves were adjusted so that full chamber pressure was obtained in 0.02 to 0.06 second. This "step function" in chamber pressure, or driving temperature, allowed a simple mathematical model to be used for obtaining heat-transfer coefficients.

CALCULATION PROCEDURE

Reference 8 shows that the transient heat-conduction problem of heat flow in a composite thrust-chamber wall may be treated by the "thin" shield method. That is, with very thin thermal shielding, the problem can be reduced to a simple slab conduction problem with a reduced effective heat-transfer coefficient:

$$h_{eff} = \frac{h}{1 + \frac{ht}{k}}$$

where h is the hot-gas-side heat-transfer coefficient, and t and k are the thickness and conductivity of the thermal shield. (Symbols are also defined in the appendix.) Therefore, with this equation, the effective heat-transfer coefficients measured in each of the coated sectors along with the corrected heat-transfer coefficient obtained from the uncoated sector gave a value of t/k for each sector. Then, with the known thickness of the coating applied to each sector, a value of the effective conductivity could be obtained for each sector. This equation assumes that the heat-transfer coefficient of the uncoated sector is not a function of the wall temperature and also assumes that there is no circumferential variation of the heat-transfer coefficient. The hot-gas-side heat-transfer coefficient from the uncoated sector as used in the equation is thus, in reality, substituted for the hot-gas-side heat-transfer coefficient to which the coated sector is subjected. Roughness differences between the uncoated and coated sectors could affect the heat-transfer coefficient and cause error in obtaining the effective thermal conductivity. In order to ensure good mechanical contact between a coating and the thrust-chamber surface, the entire copper surface was blasted with #60 aluminum oxide (Al_2O_3) grit. A surface roughness of 3.175 rms micrometers (125 rms μin.) was obtained. The surface roughness of the coatings used was measured to be 3.302 rms micrometers (130 rms μin.). This difference in surface roughness should not have affected the results. The original copper surface had a 1.6256-rms-micrometer (64-rms-μin.) surface roughness.

During the tests, some coatings were lost at measuring stations. When this happened, the heat-transfer coefficients from these tests (3.048 rms μm; 120 rms μin.) were found to be the same as those obtained previously in references 6 and 7 (1.6256 rms μm; 64 rms μin.). This was also true for the uncoated sector.

These results also proved that the addition of the small film-cooling holes at the outer circumference of the injector did not cause errors at the measuring stations.

Since the thrust chambers used in these tests were the same as those used in references 6 and 7, the circumferential variation was known, and correlations had already been obtained for the heat-transfer coefficients for the uncoated thrust chambers. Therefore, the uncoated heat-transfer coefficient could be corrected for wall temperature by using the correlations previously obtained and putting in the gas transport properties at the right reference enthalpy (i. e., using the correct wall temperature). This is an iteration process. However, one iteration was considered sufficient.

No circumferential variation of the heat-transfer coefficient was taken into account, since reference 7 showed that the instrument stations 180° apart in the chamber had no variation. At the throat, the variations were random. Therefore, the complete composite coating was always applied to the sector 180° from the uncoated sector, and no circumferential correction was necessary. Since the conductivity values of the other layers are only useful in getting a qualitative understanding of how to design an effective coating, no corrections were applied.

The effective heat-transfer coefficients of the coated sectors and the heat transfer coefficients of the uncoated sector were obtained by using the constant-h method explained in detail in reference 6.

RESULTS AND DISCUSSION

Analysis of the Thrust-Chamber Design Problem Using Coatings

Before the discussion of the results of these tests, a brief analysis will be presented to give the reader an insight into the effective use of coatings. The effective use of coatings in the design of a thrust chamber requires a knowledge of the effective conductivity k of the coating system to be used. Also required is the ability to select the correct coating thickness for the particular heat flux level that must be cooled at each axial station.

In order to get an insight, a graphical representation (fig. 7) was made which shows how a composite figure will finally be put together to analyze coatings. Figure 7(a) is a sketch of the effective heat-transfer coefficient as a function of the hot-gas-side heat-transfer coefficient for various coating resistances t/k. Thus, figure 7(a) is just a graphical representation of the equation

$$h_{eff} = \frac{h}{1 + \frac{ht}{k}}$$

Then, if values are selected for the driving temperature T_{aw} and the metal/coating interface temperature T_{uw}, lines of equal heat flux q can be added (fig. 7(b)) by the use of the equation $q = h_{eff}(T_{aw} - T_{uw})$ and various values of h_{eff}. Finally, lines for the coating surface temperature T_{gw} can be added by using the equation

$$h_{eff} = \frac{h(T_{aw} - T_{gw})}{T_{aw} - T_{uw}}$$

These lines are shown in figure 8 along with the t/k and q lines from the preceding steps. For figure 8, a value of k = 2.24 watts per meter kelvin (0.3×10^{-4} Btu/(in.)(sec)(^{o}R)) was chosen. This is a representative number for the composites tested in this investigation. Since the driving temperature T_{aw} does not vary too much through the critical design region, a driving temperature can be assumed. For these two plots of figure 8, a driving temperature of 3333 K (6000^{o} R) was chosen. The next parameter to be assumed was the temperature of the interface between the coating and the metal wall, T_{uw}. For a high heat flux design, one could choose the maximum wall temperature that the metal could tolerate, or a lower temperature could be chosen in order to ensure a long thermal-fatigue cyclic life for the metal for a noncritical design. For figure 8(a), a T_{uw} value of 1111 K (2000^{o} R) was chosen, and for figure 8(b), a value of 556 K (1000^{o} R) was chosen. For illustrative purposes, q levels of 8.17×10^{6}, 16.342×10^{6}, and 24.513×10^{6} watts per square meter (5, 10, and 15 Btu/(in.^{2})(sec)) have been drawn on each figure (a horizontal line is a line of equal q). Lines representing coating surface temperature T_{gw} values of 1944, 2222, and 2500 K (3500^{o}, 4000^{o}, and 4500^{o} R) also have been drawn on each figure. This completes the construction needed to analyze coating thickness as a function of k, T_{aw}, T_{uw}, and T_{gw} throughout the rest of this report.

Now, for an example, suppose one decides that the coating can tolerate a temperature of 2222 K (4000^{o} R). If h is 8.824×10^{3} watts per square meter kelvin (0.003 Btu/(in.^{2})(sec)(^{o}R)), then the coating thickness should be 0.254×10^{-3} meter (0.010 in.), and the coolant passage would have to be designed to pick up a q of 9.80×10^{6} watts per square meter (6 Btu/(in.^{2})(sec)), as indicated by point A in figure 8(a). The q to which this particular station would be subjected if there were no coating and h remained constant would be 19.610×10^{6} watts per square meter (12 Btu/(in.^{2})(sec)), as indicated by point B in figure 8(a). This, of course, means the temperature difference ($T_{uw} - T_{cw}$) across the metal would double. If one had decided to use a lower metallic wall temperature, say T_{uw} = 555 K (1000^{o} R), to reduce thermal fatigue and increase cyclic life, but with the same coating temperature of 2222 K (4000^{o} R), the q load would still be 9.80×10^{6} watts per square meter (6 Btu/(in.^{2})(sec)), as indicated by point C in figure 8(b). However, the thickness now needed would be 0.381×10^{-3} meter (0.015 in.); and if

the coating were lost, q would be 24.513×10^6 watts per square meter (15 Btu/(in.^{2})(sec)), as indicated by point D in figure 8(b). The preceding examples show the designer how to construct curves for his coating system and then choose values of thicknesses for the various q levels at the various axial stations.

These figures also point out dramatically (what the equation $h_{eff} = h/[1 + (ht/k)]$ shows) that for a given k and t, the higher the h, the more effective the coating becomes (h_{eff}/h becomes smaller). Also, if one can design in the region where the t curves are flat, the values of h can vary over quite a range without greatly affecting the q level, because h_{eff} remains nearly constant. The temperature of the coating does increase or decrease, though, as h varies up or down. Thus, the coating temperature T_{gw}, if designed to be a conservative value, can be the safety valve that allows q to effectively remain the same while the h varies considerably. For example, suppose that h is 12.8×10^3 watts per square meter kelvin (0.00435 Btu/(in.^{2})(sec)($^\circ$R)) for a T_{gw} of 2222 K (4000° R) and a thickness of 0.254×10^{-3} meter (0.010 in.), as illustrated by point E in figure 8(b). If for some reason h goes to 20×10^3 watts per square meter kelvin (0.0068 Btu/(in.^{2})(sec)($^\circ$R)), a 37-percent change, the T_{gw} goes to 2500 K (4500° R), a 12.5-percent change, as illustrated by point F in figure 8(b). However, the q level only changes from 14.218×10^6 to 16.67×10^6 watts per square meter (8.7 to 10.2 Btu/(in.^{2})(sec)), a 17.3-percent change. In reality, since the above example was in an area where the t curves were not exactly flat, T_{uw} would change a small amount, and a new heat balance would have to be made. Thus, a new plot would have to be made with the new T_{uw} parameter. For an uncoated case, this would have been a change in q from 35.54×10^6 to 55.5×10^6 watts per square meter (21.75 to 34 Btu/(in.^{2})(sec)), a 56.4-percent change. The heat-transfer coefficient for a given design is usually predictable to within ±15 percent. Therefore, the above example and figure 8 give a designer a feel for the sensitivity of various parameters involved with coatings.

Experimental Results and Discussion

Composite type 2 coating as designed was made up of five layers. Layer 1 was a 0.508×10^{-4}-meter (0.002-in.) coating of molybdenum (Mo). Layer 2 was made up of a 0.508×10^{-4}-meter (0.002-in.) coating of 83.2 percent by weight of Mo and 16.8 percent by weight of zirconium oxide (ZrO_2) stabilized with calcium oxide (CaO). Layer 3 was a 0.508×10^{-4}-meter (0.002-in.) coating comprised of 62.5 percent by weight of Mo and 37.5 percent by weight of ZrO_2. Layer 4 was a 0.508×10^{-4}-meter (0.002-in.) coating of 35.5 weight percent Mo and 64.5 weight percent ZrO_2. Layer 5 was a 1.016×10^{-4}-meter (0.004-in.) layer of 64.3 percent hafnium oxide (HfO_2) by weight and 35.7 percent

ZrO_2 by weight. Table I(a) gives these data and also the as-sprayed thickness data. The actual as-sprayed thickness obtained from photomicrographs was used in all calculations.

Figure 9 shows a plot of the effective conductivity as a function of average coating temperature for coating composite type 2. Average coating temperature is the arithmetic average of T_{uw} and T_{gw}. The three points of data for each layer at each station are three cuts in time during the transient test. The data for all stations are not always given because the coatings were lost at some positions. The following are some causes of coating loss: (1) movement of the rods with respect to the thrust chamber wall due to differential expansion during heating and differential contraction from cooling (the rod receives heat from a one-dimensional process, while the wall receives heat from a three-dimensional process); (2) uncleanliness of subsurface; (3) improper subsurface treatment; and (4) rods are threaded into the wall, and after many runs, some rods develop leaks from engine vibration. Nitrogen pressurizing gas is also used in the cavities. The coatings, in general, adhere to the main engine wall much better than at rod locations.

Table IV shows the bulk conductivities and the 37-percent-porous conductivities of a number of materials. These are approximate conductivities at temperatures of 1111 to 1667 K (2000° to 3000° R) taken from references 9 and 10. The 37-percent-porosity values are given because this was the average porosity found from nine photomicrographs of the coated shields from three different thrust-chamber coatings. Where values of conductivity for 37-percent-porous materials could not be found in the literature, a value of 22 percent of the bulk conductivity was used. This value of 22 percent was obtained from the porous-metal work of reference 11. Table IV shows that for the two main materials (Mo and ZrO_2) used in coating composite type 2, the conductivity of 37-percent-porous Mo is approximately 25 times that of 37-percent-porous ZrO_2. One would expect the conductivities of the first layer to be higher than those of the second layer, and those of the second to be higher than those of the third, etc. However, the data of figure 9 indicate that this is not so. In fact, the data all fall in a band from 1.046 to 4.782 watts per meter kelvin (0.14×10^{-4} to 0.64×10^{-4} Btu/(in.)(sec)($^{\circ}$R)).

In order to determine the effective thermal conductivities of the various layers, calculations were performed with the use of a porosity of 37 percent and various models. The Lichtenecker formula model for mechanical mixtures with no solubility and no chemical reaction is

$$k_{eff} = k_1^{V_1} \cdot k_2^{(1-V_1)}$$

where k_{eff} is the thermal conductivity of the mixture, k_1 and k_2 are the thermal conductivities of the components 1 and 2, respectively, and V_1 is the volume fraction of

component 1. The relation between volume fraction and weight fraction is

$$W_1 = \frac{V_1\rho_1}{\rho_2(1 - V_1) + V_1\rho_1}$$

where W_1 is the weight fraction of component 1, and ρ_1 and ρ_2 are the densities of components 1 and 2, respectively. This model was used to get the effective conductivities of the various layers. These layers were then put together by using the following equation for the composite layers:

$$\frac{t_{composite}}{k_{composite}} = \frac{t_{1e}}{k_{1e}} + \frac{t_{2e}}{k_{2e}} + \frac{t_{3e}}{k_{3e}} + \ldots + R$$

Figure 10 shows plots of t/k against t for the data for composite coating type 2 for the chamber and throat axial stations. Lines of constant k are also shown. The lines predicted by the Lichtenecker model for the coating thickness obtained from photomicrographs are shown on these plots with thermal contact resistance R (changes due to spraying) equal to zero. The other two lines of these plots were calculated by using the results obtained from references 2 and 3. The data in figure 10 do not agree with the predictions of the Lichtenecker model or the results from references 2 and 3. In fact, R cannot be considered zero and, instead, the effective conductivity agrees with the results of reference 4, wherein contact resistance is hypothesized as being the controlling factor. The chamber data in figure 10(a) seems to have the same shape as the model predicts but with much higher values of t/k. This is not true for the data of figure 10(b). The scatter of the data could be due to differences in contact resistance. Barzelay et al. (ref. 12) in their report on contact resistances found that for extremely smooth and flat surfaces in contact, the conductance values were highly sensitive to minute changes in the matching configurations and varied widely. For example, in a test of two different pairs of specimens of the same roughness, they found conductances five to six times as high as in the normal case. They concluded that it was possible, apparently without any special care, to match at least one specimen pair to such near perfection that the high conductances were attained. In another series of tests conducted with an assembly of dissimilar materials, they found results difficult to explain. The first arrangement of this type consisted of an aluminum alloy in contact with stainless steel, with heat flowing from the aluminum alloy to the steel. This was followed by a second series of tests, without outwardly disturbing the interface assembly, where the specimen pair was inverted so that the heat now flowed from the stainless steel to the aluminum specimen. They found that the same interface presented greatly different thermal resistances for the two different directions of heat flow, with the first arrange-

ment giving conductance values several times higher than the second. They theorized that warping, which was an important factor in determining the conductance, was a function of the temperature level and that the top specimen, in contact with the heating element, must obviously be at a higher temperature than the mean interface temperature; conversely, the bottom specimen, in contact with the cooling element, is always at a lower temperature than the mean interface temperature. Therefore, for a given interface temperature, the mean temperatures of the two individual specimen blocks are always substiantially different, depending on their position, top or bottom, with respect to the direction of heat flow. The discussion of results in reference 12 contains the following statements:

(1) The mechanism of heat transfer across surfaces in contact is exceedingly complex.

(2) The great number of interrelated factors make it difficult, if not impossible, to establish a clear-cut cause-and-effect relation experimentally.

(3) From the point of view of obtaining results useful in actual design, only limited success has been obtained, since the conductance values measured cannot be precisely duplicated without duplicating the experimental conditions.

Tests (unpublished) of zirconium carbide (ZrC) conducted at Los Alamos Laboratories showed that the conductivity of 37-percent-porous material had been reduced from 2.39×10^6 to 0.37×10^6 watts per meter kelvin (32 to 5 Btu/(in.)(sec)($^\circ$R)). Such a large reduction in conductivity could not be explained simply by the addition of pores. The low values were explained by poor bonding of the grains, resulting in contact resistance across the grain boundaries. These tests at Los Alamos Laboratories also showed that the conductivity of ZrO_2 could be reduced by increased porosity, but not to the same extent as reported for ZrC. At 30-percent porosity, the conductivity of ZrO_2 was reduced from 2.08×10^4 to 0.865×10^4 watts per meter kelvin (1.2 to 0.5 Btu/(ft)(hr)($^\circ$R)).

Going back to figure 9, one also sees that changing the percentage of hydrogen does not seem to affect the conductivity within the accuracy of the data. The solid symbols and the tailed symbols indicate 25 and 15.6 percent hydrogen, respectively, while the main data were obtained with 17.7 percent hydrogen. The data, therefore, show that the entrained gas does not seem to affect the value of conductivity. Furthermore, the scatter of the data is such that, within the accuracy obtainable with the rocket firing, the temperature of the coating has no apparent effect on the conductivity.

Figure 11 shows the data for Cu III with this same coating. These data are for chamber pressures of 4.137×10^6 and 6.20×10^6 newtons per square meter absolute (600 and 900 psia). All the data are for the composite of five layers. The numbers indicate the axial stations where data were obtained. Figure 11 seems to indicate that conductivity falls off as temperature increases. But actually, the spread of the data with stations is such that really only the spread in data is indicated with k varying from a value

of 1.05 to 7.47 watts per meter kelvin (0.14×10^{-4} to 1×10^{-4} Btu/(in.)(sec)(^{o}R)). The data also indicate that chamber pressure does not seem to have any effect on the conductivity of the coating.

Figure 12 shows k as a function of $\overline{T}_{ct}$ for composite coating type 3. Figure 13 is a plot of t/k as a function of t for the same coating. Table I(b) gives the details of this five-layer composite. Both these figures indicate that at station 1 (fig. 13(a)) a constant k is representative for all layers, as well as for the five-layer composite. The throat data (fig. 13(b)), however, indicate that the conductivities of the more metallic layers are indeed higher than the more ceramic layers. The photomicrographs of this coating composite are given in figure 3. The bondings of the coatings to the copper substrate evidently have a purely mechanical character. The particles are wedged in the surface irregularities, fill up the depressions, and do not have a continuous close contact with the substrate. The particles are deposited on each other at random, thereby forming numerous pores. The layers are composed of individual or partly welded flattened droplets and have a laminated structure. Therefore, it is indeed not surprising that there is much scatter in the data, as the photomicrographs clearly show that contact resistance between the grains and the substrate should clearly influence the effective thermal conductivity.

Figure 14 shows k as a function of $\overline{T}_{ct}$ for layered coating type 5. Figure 15 is a plot of t/k as a function of t for the same coating. The results for a type 6 coating are shown in figure 16. Here again, the results are shown to be repeatable by a subsequent run, as was the case with previous coatings. The data show a wide spread in values of k, but again, the supposedly most conductive layer shows about the same value of k as the succeeding layer. The values of k are much lower than those expected on the basis of table IV.

The results of all the tests indicate that the spread of data is large. If all data for the complete composites were averaged, a value of 3 watts per meter kelvin (0.4×10^{-4} Btu/(in.)(sec)(^{o}R)) would be obtained. In other words, the thermal contact resistances between the grain boundaries of a coating essentially determine its total thermal resistance. Thus, the values of the thermal conductivities of the grains themselves, which are different for different materials, have little effect on the thermal conductivity of the coating.

Reference 1 quotes the conductivities of a group of samples. Table V lists the compositions and the values of conductivity for a few of these samples. These values from reference 2 approximately agree with the values obtained in the present tests and also show that the materials used do not greatly change the value of conductivity obtained. Therefore, although the spread in the present data is large, the data seem to indicate the approximate values of k for all coatings are around 3 watts per meter kelvin (0.4×10^{-4} Btu/(in.)(sec)(^{o}R)), with maybe a 3- or 4-to-1 variation, depending on mate-

rials used, instead of the 20- or 30-to-1 variation that might be expected on the basis of the conductivity values of table IV.

The value of 3 watts per meter kelvin (0.4×10^{-4} Btu/(in.)(sec)(^{o}R)) for conductivity does provide a very effective thermal barrier for rocket applications, as shown by figures 7 and 8, which were constructed with a value for k of 2.242 watts per meter kelvin (0.3×10^{-4} Btu/(in.)(sec)(^{o}R)).

CONCLUSIONS

The following conclusions were drawn on the basis of this investigation of the effective thermal conductivities of four metal-ceramic gradated coatings plasma-arc-sprayed on hydrogen-oxygen thrust chambers:

1. Within the accuracy and range of the present tests, the thermal conductivities of the composite coatings are not functions of pressure.

2. Within the accuracy and range of the present tests, the thermal conductivities of the composite coatings are not functions of the percentage of hydrogen, and thus the entrained gas in the porous ceramic does not seem to affect the value of conductivity.

3. The conductivities of the various composites tested all fell in the range of approximately 0.75 to 7.5 watts per meter kelvin (0.1 to 1.0×10^{-4} Btu/(in.)(sec)(^{o}R)), with the bulk of the data at about 3 watts per meter kelvin (0.4×10^{-4} Btu/(in.)(sec)(^{o}R)).

4. The various materials that made up any specific composite do not seem to affect the thermal conductivity values as much as the difference in the thermal conductivities of the bulk materials would lead one to expect.

5. Thermal contact resistance between substrate interface and between grain boundaries has a major influence on the effective thermal conductivities of coatings.

6. The thermal conductivities of the coatings are such that they can be used to provide very effective thermal barriers.

CONCLUDING REMARKS

The temperature difference across a coating is usually taken as a measure of the thermal shock resistance of a coating of a given thickness. Previous to the present work, the design theory has been that the thickness of a coating used as a thermal barrier had to be increased as metals were added as components to the coating, because the conductivity was expected to increase. This is still true, but the conductivity changes are much smaller than would be expected on the basis of the conductivities of the bulk materials. Since the thermal shock resistance is also a function of Biot's modulus, ht/k, the thinner coatings should be more shock resistant.

The results of the present investigation indicate that more tests are required with much greater amounts of high-conductivity materials in the lower layers of the composites. The reason for low values of conductivity is that the grains and substrate interface are not well bonded. This results in contact resistance across grain boundaries. Therefore, more laboratory work is needed to develop coatings (for intermediate layers) which will provide higher values of conductivity. If coatings are to be used at higher and higher levels of heat flux for the same temperature difference across the coating, the thicknesses will decrease, and very sophisticated techniques of applying these coatings or coatings with higher conductivities will be required.

Since these were only short tests, longer duration tests with coatings on cooled tubes must be made to determine the effects of temperature cycling and time on the durability of the coatings.

The conclusions and remarks of this report must be restricted to gradated coatings derived from plasma spraying. The effective conductivities presented herein must also be restricted to uses similar in application to those of this report.

Lewis Research Center,
National Aeronautics and Space Administration,
Cleveland, Ohio, August 30, 1972,
503-35.

APPENDIX - SYMBOLS

A	cross-sectional area
A^*	throat cross-sectional area
D	density of individual components making up coating
h	heat-transfer coefficient
ht/k	Biot number
k	thermal conductivity
L^*	characteristic length of rocket thrust chamber
P	pressure
q	heat flow rate per unit area
R	thermal contact resistance
T_{aw}	adiabatic wall temperature
$\overline{T}_{ct}$	average coating temperature, $(T_{uw} + T_{gw})/2$
T_{cw}	coolant-side wall temperature
T_{gw}	coating surface temperature
T_{uw}	temperature of interface between wall metal and coating
t	coating thickness
V	volume fraction
w	weight fraction
x	axial distance from throat
θ	angular position
ρ	density
Subscripts:	
B	bulk
c	chamber
eff	effective
p	porous
1	component 1
2	component 2
1e, 2e, etc.	first layer, second layer, etc.

REFERENCES

1. Stubbs, V. R.: Development of a Thermal Barrier Coating for Use on a Water-Cooled Nozzle of a Solid Propellant Rocket Motor. Aerojet-General Corp. (NASA CR-72549), May 3, 1969.

2. Lewis, W. J.: Coatings for Regenerative Engines. Rep. 28238T, Aerojet-General Corp. (NASA CR-72413), July 12, 1968.

3. Lewis, W. J.: Coatings for Advanced Thrust Chambers. Aerojet-General Corp. (NASA-CR-72604), c. 1968.

4. Boganov, A. G.; Pirogov, Yu. A.; and Makarov, L. P.: Investigation of the Effective Thermal Conductivity and Total Emissivity of Heat-Resistant Ceramic Coatings of Refractory Oxides Produced by Gas-Flame Spraying. High Temp., vol. 3, no. 1, Jan.-Feb. 1965, pp. 53-58.

5. Curren, Arthur N.; Grisaffe, Salvatore J.; and Wycoff, Kurt C.: Hydrogen Plasma Tests of Some Insulating Coating Systems for the Nuclear Rocket Thrust Chamber. NASA TM X-2461, 1972.

6. Schacht, Ralph L.; Quentmeyer, Richard J.; and Jones, William L.: Experimental Investigation of Hot-Gas Side Heat-Transfer Rates for a Hydrogen-Oxygen Rocket. NASA TN D-2832, 1965.

7. Schacht, Ralph L.; and Quentmeyer, Richard J.: Axial and Circumferential Variations of Hot-Gas-Side Heat-Transfer Rates in a Hydrogen-Oxygen Rocket. NASA TN D-6396, 1971.

8. Lin, C.-C., ed.: Turbulent Flows and Heat Transfer. Vol. V of High Speed Aerodynamics and Jet Propulsion. Princeton Univ. Press, 1959.

9. Touloukian, Y. S., ed.: Thermophysical Properties of High Temperature Solid Materials. Macmillan Co., 1967.

10. Tebo, F. J.: Selected Values of the Physical Properties of Various Materials. Rep. ANL-5914, Argonne National Lab., Sept. 1958.

11. Grootenhuis, P.; Powell, R. W.; and Tye, R. P.: Thermal and Electrical Conductivity of Porous Metals Made by Powder Metallurgy Methods. Proc. Phys. Soc., Sec. B, vol. 65, pt. 7, July 1952, pp. 502-511.

12. Barzelay, Martin E.; Tong, Kin Nee; and Holloway, George F.: Effect of Pressure on Thermal Conductance of Contact Joints. NACA TN 3295, 1955.

TABLE I. - COMPOSITIONS AND THICKNESSES OF COATING LAYERS ON THRUST CHAMBER Cu II

(a) Composite coating type 2 (readings 123, 126, and 129)

Radial locations of layers in thrust chamber

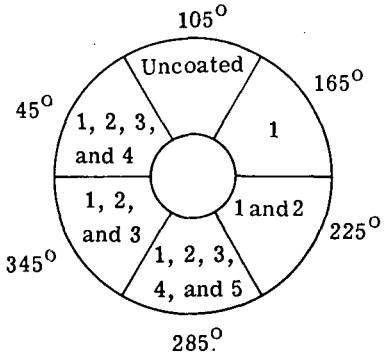

Layer	Thickness		Composition, wt. %
	mm	in.	
1	0.0508	0.002	100 Mo
2	0.0508	0.002	83.2 Mo - 16.8 ZrO_2 stabilized with CaO
3	0.0508	0.002	62.5 Mo - 37.5 ZrO_2 stabilized with CaO
4	0.0508	0.002	35.5 Mo - 64.5 ZrO_2 stabilized with CaO
5	0.1016	0.004	64.3 HfO_2 - 35.7 ZrO_2 stabilized with CaO

Layers	Cumulative thickness											
	Design		Measured									
	mm	in.	mm	in.	mm	in.	mm	in.	mm	in.	mm	in.
			Measuring station 1 (A/A* = 4.64)		Measuring station 2 (A/A* = 1.78)		Measuring station 3 (A/A* = 1.00)		Measuring station 4 (A/A* = 1.27)		Measuring station 5 (A/A* = 3.33)	
1	0.0508	0.002	0.0508	0.002			0.0508	0.002				
1 and 2	0.1016	0.004	0.2032	0.008			0.1016	0.004				
1, 2, and 3	0.1524	0.006	0.2540	0.010			0.1270	0.005				
1, 2, 3, and 4	0.2032	0.008	0.2794	0.011			0.2032	0.008				
1, 2, 3, 4, and 5	0.3048	0.012	0.3048	0.012	0.2540	0.010	0.229	0.009	0.2032	0.008	0.229	0.009

TABLE I. - Continued. COMPOSITIONS AND THICKNESSES OF COATING LAYERS

ON THRUST CHAMBER Cu II

(b) Composite coating type 3 (readings 166 and 169)

Radial locations of layers in thrust chamber

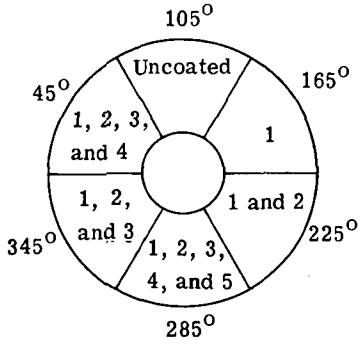

Layer	Thickness		Composition, wt. %
	mm	in.	
1	0.0508	0.002	100 Mo
2	0.0508	0.002	80 Nichrome - 20 Al_2O_3
3	0.0508	0.002	30 Nichrome - 70 Al_2O_3
4	0.0508	0.002	10 Nichrome - 90 Al_2O_3
5	0.1016	0.004	100 Al_2O_3

Layers	Cumulative thickness											
	Design		Measured									
	mm	in.	mm	in.	mm	in.	mm	in.	mm	in.	mm	in.
			Measuring station 1 (A/A^* = 4.64)		Measuring station 2 (A/A^* = 1.78)		Measuring station 3 (A/A^* = 1.00)		Measuring station 4 (A/A^* = 1.27)		Measuring station 5 (A/A^* = 3.33)	
1	0.0508	0.002	0.0254	0.001			0.0356	0.0014				
1 and 2	0.1016	0.004	0.0660	0.0026			0.1143	0.0045				
1, 2, and 3	0.1524	0.006	0.0914	0.0036			0.1372	0.0054				
1, 2, 3, and 4	0.2032	0.008	0.1422	0.0056			0.1753	0.0069				
1, 2, 3, 4, and 5	0.3048	0.012	0.2591	0.0102	0.1803	0.0071	0.2210	0.0087	0.2032	0.008	0.2083	0.0082

TABLE I. - Continued. COMPOSITIONS AND THICKNESSES OF COATING LAYERS

ON THRUST CHAMBER Cu II

(c) Layered coating type 5 (readings 177, 180, 183, and 186)

Radial locations of layers in thrust chamber

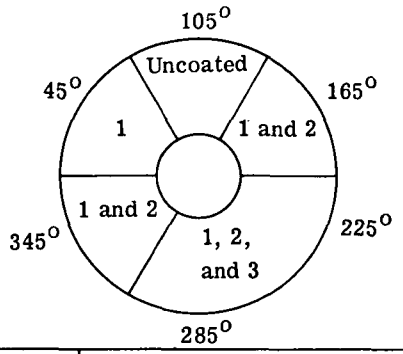

Layer	Thickness		Composition, wt. %
	mm	in.	
1	0.0508	0.003	100 Mo
2	0.0762	0.003	100 Nichrome
3	0.1016	0.004	100 ZrO_2 stabilized with CaO

Layers	Cumulative thickness											
	Design		Measured									
	mm	in.	mm	in.	mm	in.	mm	in.	mm	in.	mm	in.
			Measuring station 1 (A/A = 4.64)		Measuring station 2 (A/A = 1.78)		Measuring station 3 (A/A = 1.00)		Measuring station 4 (A/A = 1.27)		Measuring station 5 (A/A = 3.33)	
1	0.0508	0.002	0.0330	0.0013			0.0305	0.0012				
1 and 2	0.127	0.005	0.1016	0.004			0.0838	0.0033				
1 and 2	0.127	0.005	0.1016	0.004			0.0838	0.0033				
1, 2, and 3	0.229	0.009	0.1727	0.0068	0.1321	0.0052	0.1473	0.0058	0.1499	0.0059	0.1372	0.0054

TABLE I. - Concluded. COMPOSITIONS AND THICKNESSES OF COATING LAYERS ON THRUST CHAMBER Cu II

(d) Composite coating type 6 (readings 201 and 204)

Radial locations of layers in thrust chamber

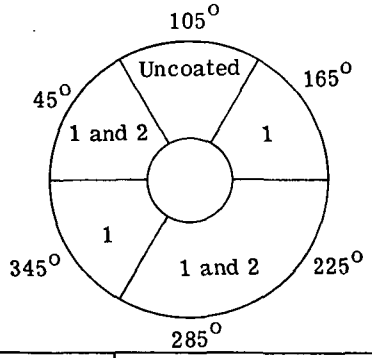

Layer	Thickness		Composition, wt. %
	mm	in.	
1	0.1016	0.004	95 W - 5 Nicoro 80
2	0.5080	0.020	85 W - 3 Cu - 12 ZrO_2 stabilized with CaC

Layers	Cumulative thickness											
	Design		Measured									
	mm	in.	mm	in.	mm	in.	mm	in.	mm	in.	mm	in.
			Measuring station 1 (A/A^* = 4.64)		Measuring station 2 (A/A^* = 1.78)		Measuring station 3 (A/A^* = 1.00)		Measuring station 4 (A/A^* = 1.27)		Measuring station 5 (A/A^* = 3.33)	
1	0.1016	0.004	0.1067	0.0042			0.1219	0.0048				
1	0.1016	0.004	0.1067	0.0042			0.1219	0.0048				
1 and 2 (45°)	0.6096	0.024	0.2667	0.0105			0.3251	0.0128				
1 and 2 (225° and 285°)	0.6096	0.024	0.2667	0.0105	0.2261	0.0089	0.3251	0.0128	0.2769	0.0109	0.1702	0.0067

TABLE II. - COMPOSITIONS AND THICKNESSES OF LAYERS OF COMPOSITE COATING TYPE 2 ON THRUST CHAMBER Cu III

[Design cumulative thickness of coating, 0.3048 mm (0.012 in.).]

Radial location of layers in thrust chamber

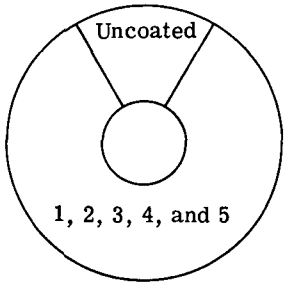

Layer	Thickness		Composition, wt. %
	mm	in.	
1	0.0508	0.002	100 Mo
2	0.0508	0.002	83.2 Mo - 16.8 ZrO_2 stabilized with CaO
3	0.0508	0.002	62.5 Mo - 37.5 ZrO_2 stabilized with CaO
4	0.0508	0.002	35.5 Mo - 64.5 ZrO_2 stabilized with CaO
5	0.1016	0.004	64.3 HfO_2 - 35.7 ZrO_2 stabilized with CaO

Measuring station		Measured cumulative thickness			
Designation	Area ratio, A/A*	mm	in.	mm	in.
		Readings 3 and 6		Readings 13, 16, and 19	
0.5	4.64	0.229	0.009	0.203	0.008
1	4.64	0.203	0.008	0.2642	0.0104
1.5	3.842	0.229	0.009	0.2616	0.0103
2	1.78	0.254	0.010	0.2718	0.0107
2.7	1.084	0.381	0.015	0.2591	0.0102
3	1.00	0.356	0.014	0.2769	0.0109
3.7	1.149	0.330	0.013	0.2261	0.0089
4	1.27	0.254	0.010	0.1981	0.0078
4.5	2.176	0.203	0.008	0.1854	0.0073
5	3.33	0.178	0.007	0.1270	0.0050

TABLE III. - ROD LOCATIONS FOR TEMPERATURE MEASUREMENTS

(a) Thrust chamber Cu II

Location designation	Axial location, x (a)		Radial location, θ	Diameter		Area ratio, A/A^*
	cm	in.		cm	in.	
1.0	-22.21	-8.744	105	27.36	10.770	4.64
			165			
			225			
			285			
			345			
			45			
2.0	-5.398	-2.125	105	16.96	6.579	1.78
2.0	-5.398	-2.125	285	16.96	6.579	1.78
3.0	0	0	105	12.70	5.000	1.00
			345			
			225			
			285			
			165			
			45			
4.0	3.810	1.5	105	14.29	5.627	1.27
4.0	3.810	1.5	285	14.29	5.627	1.27
5.0	20.39	8.026	105	23.18	9.125	3.33
5.0	20.39	8.026	285	23.18	9.125	3.33

(b) Thrust chamber Cu III

0.5	-29.49	-11.61	105	27.36	10.770	4.64
.5	-29.49	-11.61	375			
1.0	-22.21	-8.744	105			
1.0	-22.21	-8.744	375			
1.5	-13.82	-5.44	105	24.89	9.80	3.842
1.5	-13.82	-5.44	375	24.89	9.80	3.842
2.0	-5.398	-2.125	105	16.96	6.679	1.78
2.0	-5.398	-2.125	375	16.96	6.679	1.78
2.3	-3.597	-1.416	115	14.90	5.867	1.377
2.7	-1.798	-.708	395	13.22	5.205	1.084
3.0	0	0	105	12.70	5.000	1.000
3.0	0	0	375	12.70	5.000	1.000
3.3	1.270	0.500	90	12.96	5.101	1.041
3.7	2.540	1.000	345	13.61	5.359	1.149
4.0	3.810	1.500	105	14.29	5.627	1.270
4.0	3.810	1.500	375	14.29	5.627	1.270
4.5	12.10	4.763	105	18.74	7.376	2.176
4.5	12.10	4.763	375	18.74	7.376	2.176
5.0	20.39	8.026	105	23.18	9.125	3.330
5.0	20.39	8.026	375	23.18	9.125	3.330

[a]Axial locations measured relative to throat; negative values denote locations upstream of throat.

TABLE IV. - THERMAL CONDUCTIVITIES OF VARIOUS MATERIALS AT TEMPERATURES OF 1111 TO 1667 K (2000° TO 3000° R)

Material	Conductivity			
	Bulk material		37-Percent-porosity value or 22 percent of bulk value	
	W/(m)(K)	Btu/(in.)(sec)(°R)	W/(m)(K)	Btu/(in.)(sec)(°R)
Tungsten, W	107.59	14.4×10^{-4}	23.69	3.17×10^{-4}
Molybdenum, Mo	91.53	12.25	20.17	2.7
Chromium, Cr	60.52	8.1	13.30	1.78
Nichrome	26.15	3.5	5.75	.77
Aluminum oxide, Al_2O_3	8.67	1.16	3.44	.46
Zirconium oxide, ZrO_2	2.32	.3102	.773	.1034

TABLE V. - THERMAL CONDUCTIVITIES OF VARIOUS COMPOSITE SAMPLES

[Data from ref. 1.]

Sample	Composition, wt. %	Primer			Coating thickness		Surface temperature		Thermal conductivity	
		Composition	Thickness		mm	in.	K	°R	W/(m)(K)	Btu/(in.)(sec)(°R)
			mm	in.						
1	70 Al_2O_3 - 30 Mo		-----	-----	0.356	0.014	2008	3615	2.44	0.327×10^{-4}
2	70 Al_2O_3 - 30 Mo	Nichrome	0.229	0.009	.356	.014	2033	3660	2.50	.334
3	70 Al_2O_3 - 30 Mo	$NiAl_3$	.127	.005	.356	.014	2056	3700	2.50	.334
4	65 Al_2O_3 - 35 W	$NiAl_3$	.127	.005	.330	.013	2100	3780	2.25	.301
5	71 Al_2O_3 - 29 Cr	$NiAl_3$	.127	.005	.356	.014	2028	3650	2.05	.274
6	50 Al_2O_3 - 50 Mo	$NiAl_3$	.127	.005	.406	.016	2011	3620	2.95	.395
7	30 Al_2O_3 - 70 Mo	$NiAl_3$	.127	.005	.305	.012	1933	3480	2.83	.379

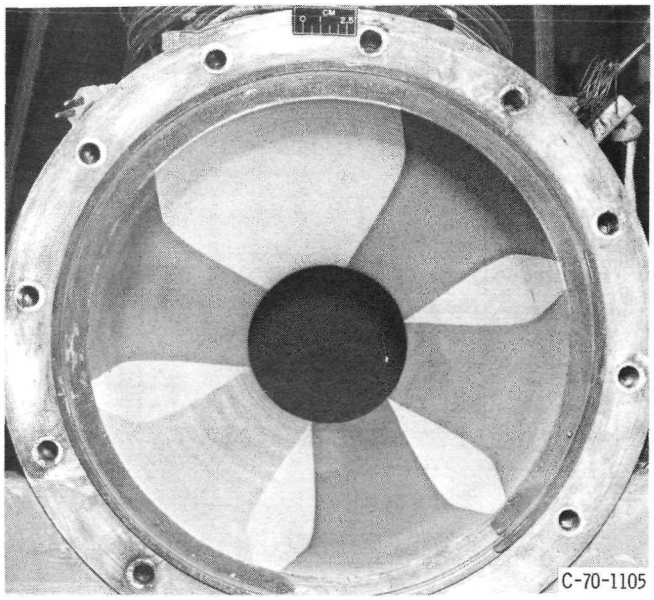

(a) Chamber end before test.

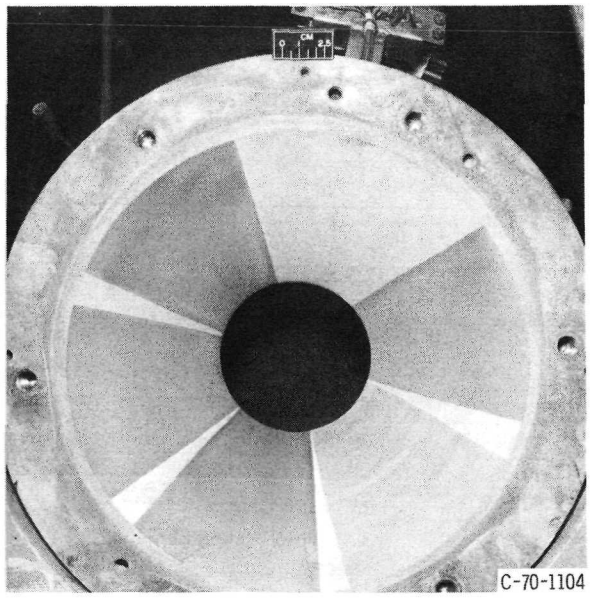

(b) Exit end before test.

Figure 1. - Typical coating pattern for thrust chamber Cu II. (Composite coating type 3.)

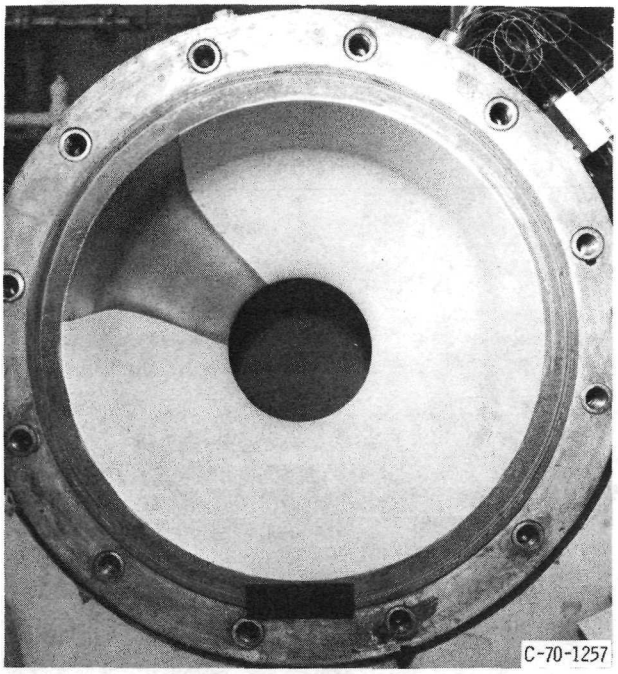

(a) Chamber end before test.

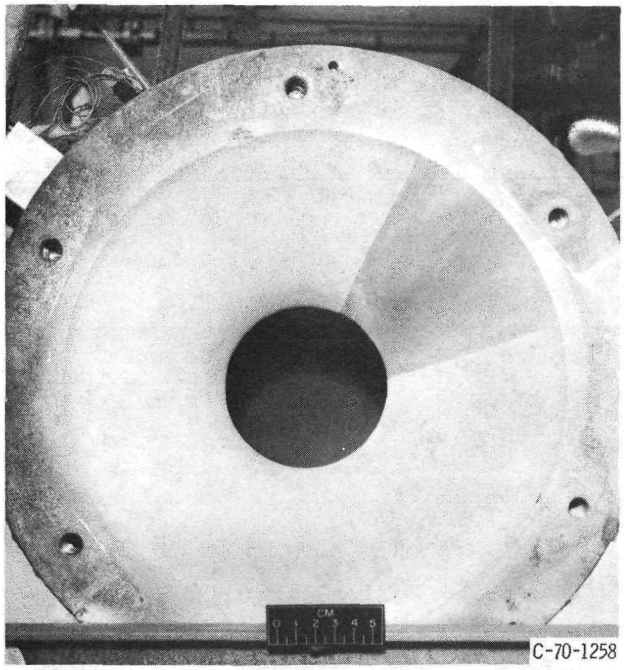

(b) Exit end before test.

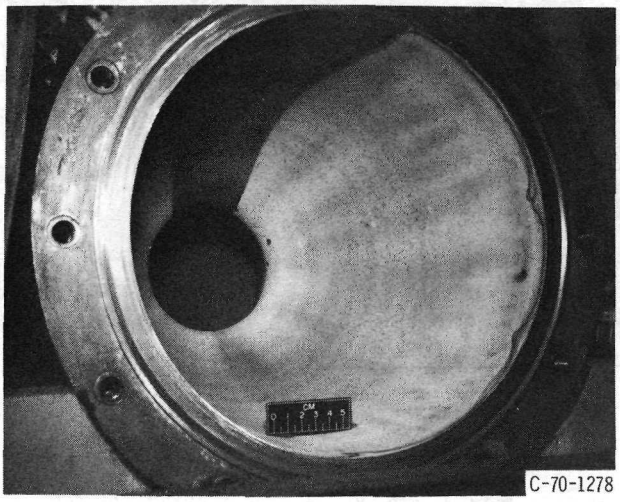

(c) Chamber end after test.

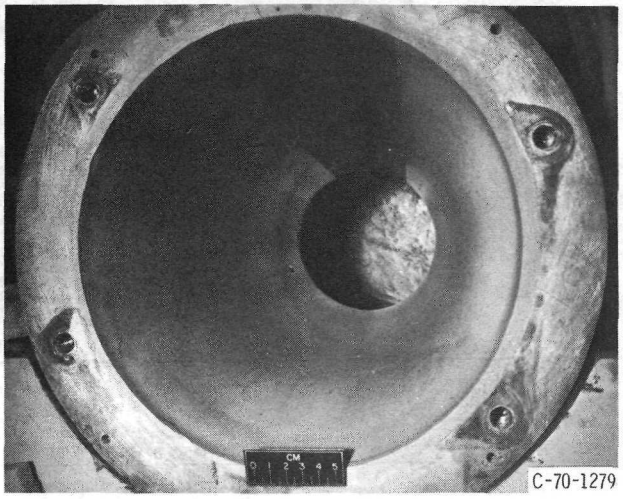

(d) Exit end after test.

Figure 2. - Typical coating pattern for thrust chamber Cu III. (Composite coating type 2.)

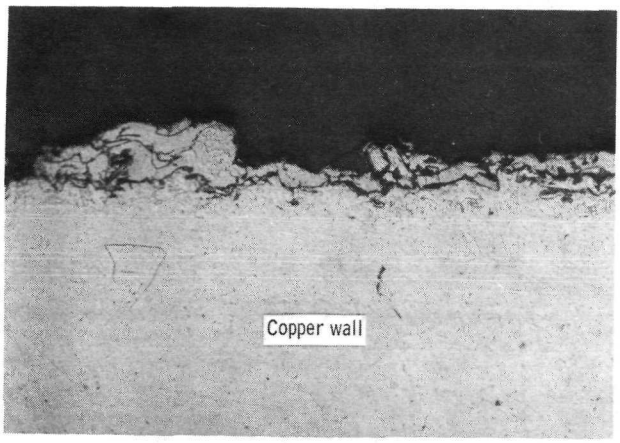

Layer 1

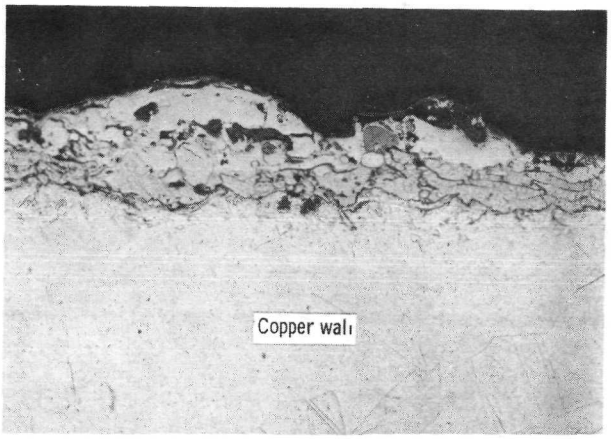

Layers 1 and 2

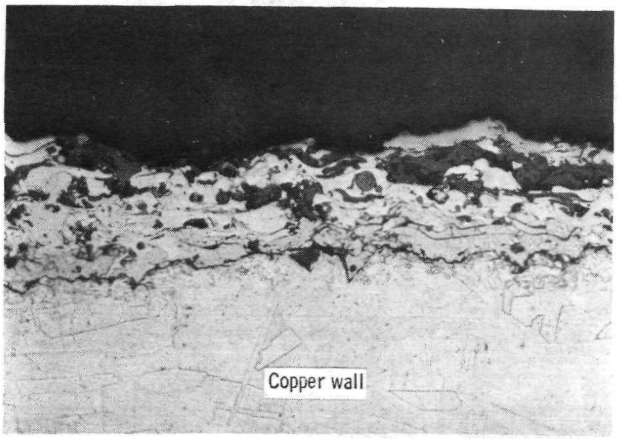

Layers 1, 2, and 3

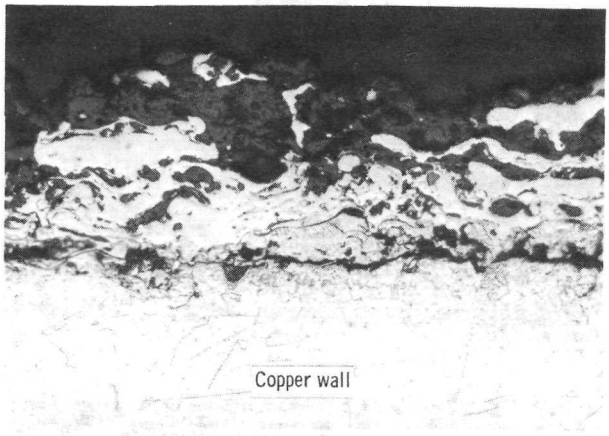

Layers 1, 2, 3, and 4

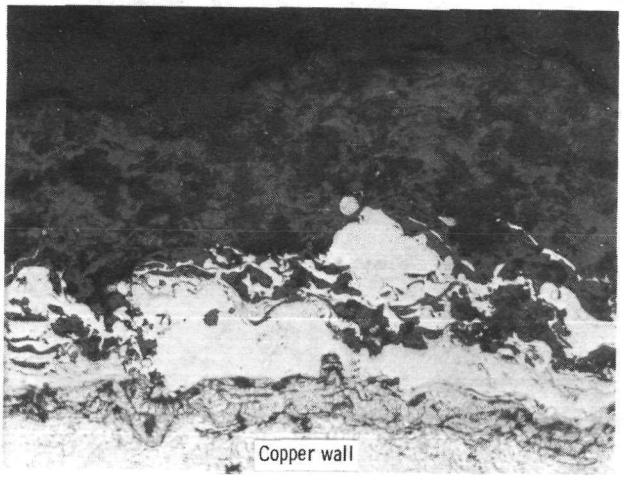

Layers 1, 2, 3, 4, and 5 (complete coating)

(a) Chamber (station 1).

Figure 3. - Photomicrographs of various layers of composite coating type 3 in thrust chamber Cu II. Composition (in wt. %) of layer 1, 100 Mo; layer 2, 80 Nichrome - 20 Al_2O_3; layer 3, 30 Nichrome - 70 Al_2O_3; layer 4, 10 Nichrome - 90 Al_2O_3; layer 5, 100 Al_2O_3. (Magnification, 250; reduced 29 percent in printing.)

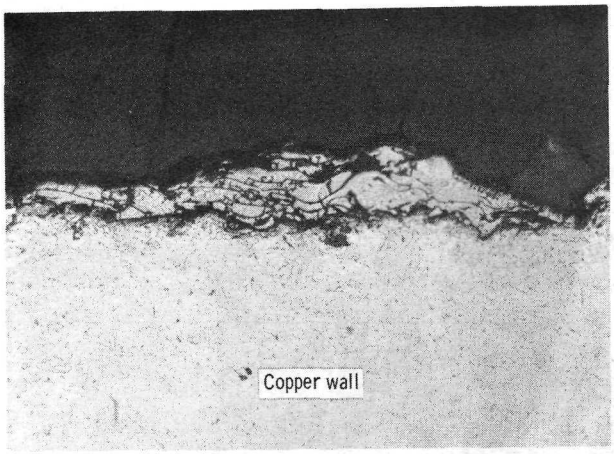

Layer 1

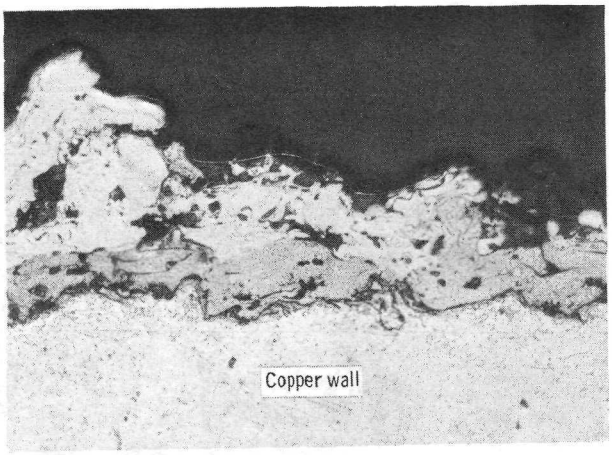

Layers 1 and 2

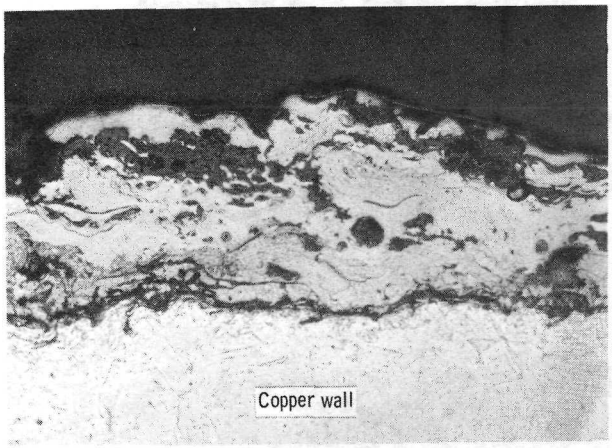

Layers 1, 2, and 3

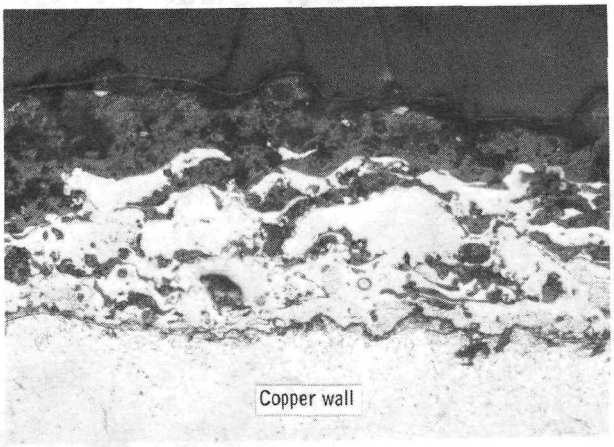

Layers 1, 2, 3, and 4

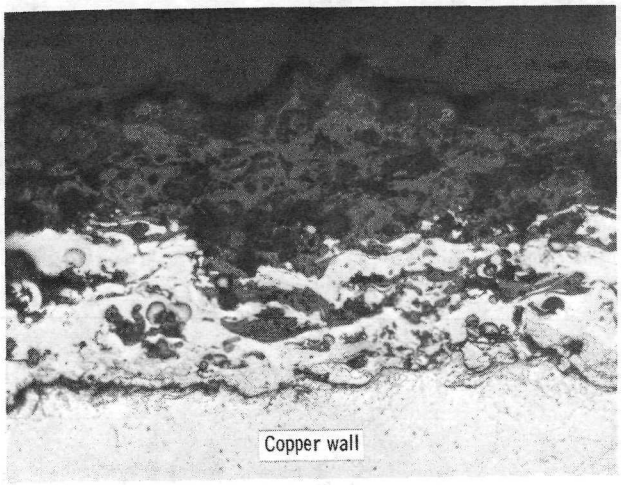

Layers 1, 2, 3, 4, and 5 (complete coating)

(b) Throat (station 3).

Figure 3. - Concluded.

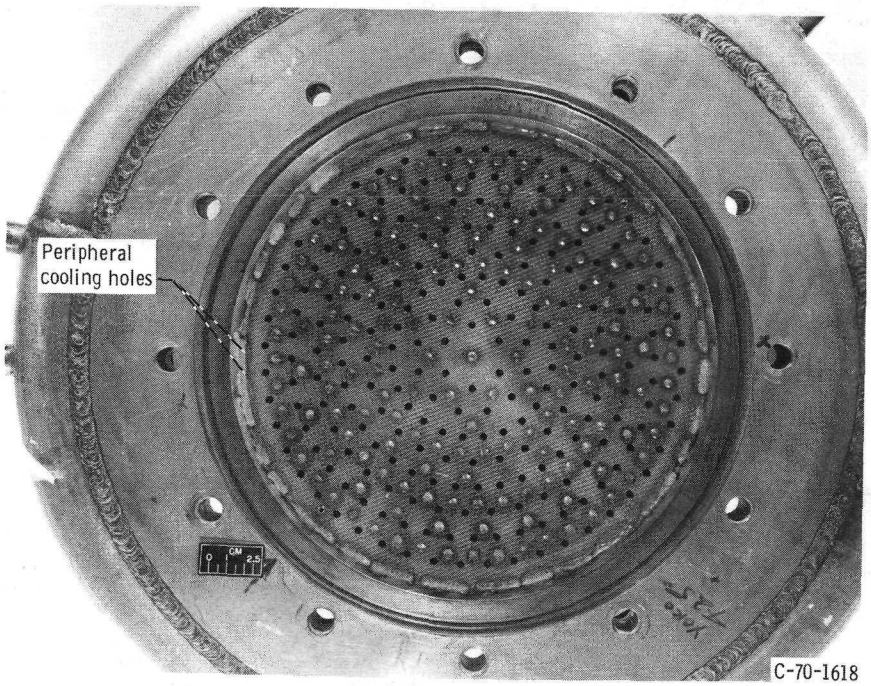

Figure 4. - Coaxial injector with porous faceplate and peripheral cooling holes.

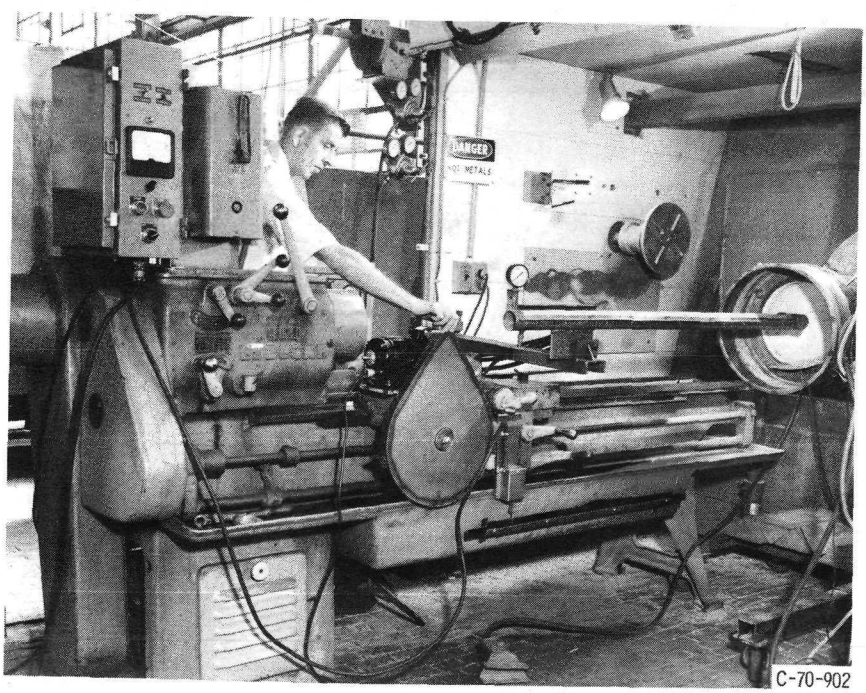

Figure 5. - Spray-coating rig.

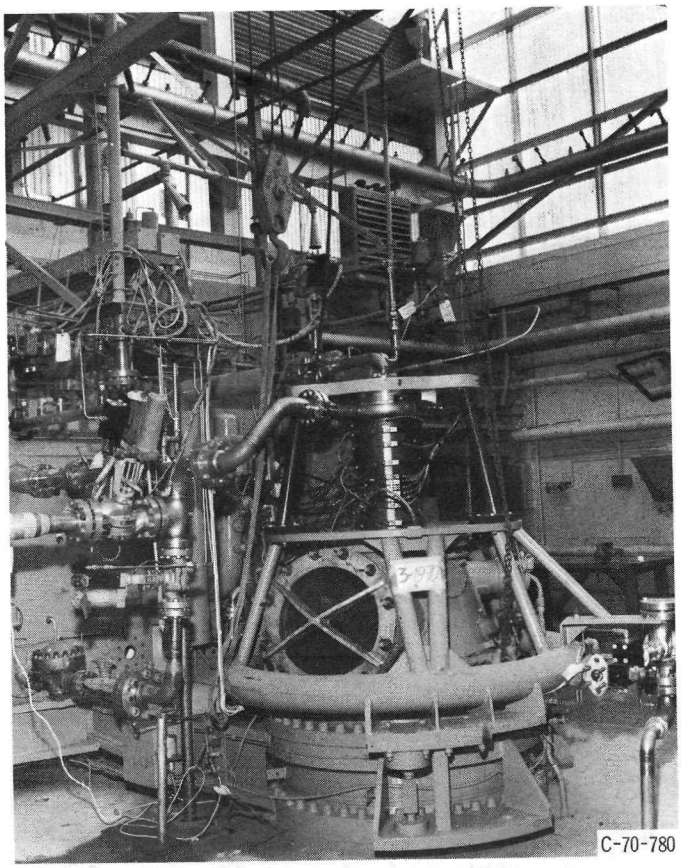

Figure 6. - Copper heat-sink rocket thrust chamber (Cu III) on test stand.

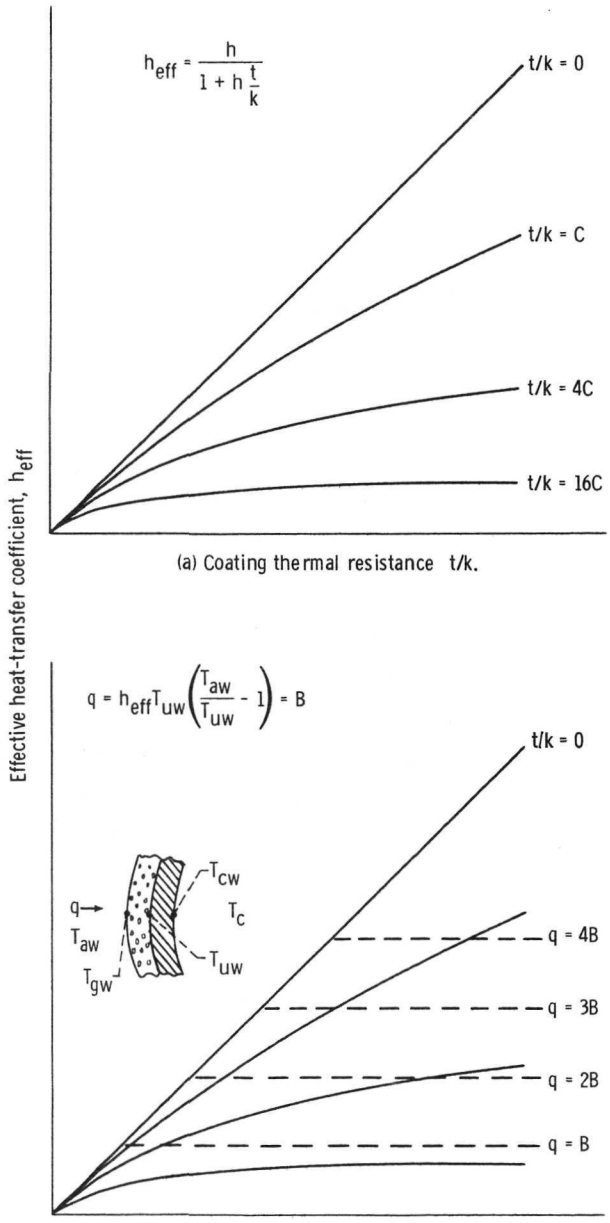

Figure 7. - Typical graphical presentation of effective heat-transfer coefficient h_{eff} as a function of hot-gas-side heat-transfer coefficient h for various levels of coating thermal resistance t/k and heat flux q.

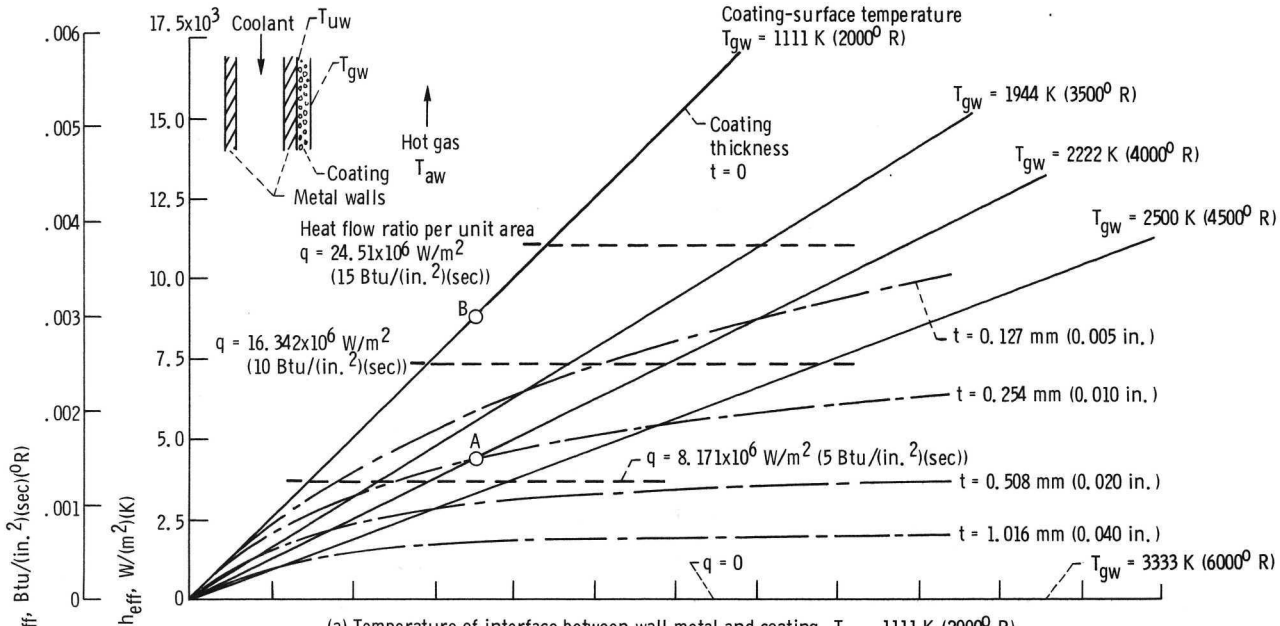

(a) Temperature of interface between wall metal and coating, T_{uw}, 1111 K (2000° R).

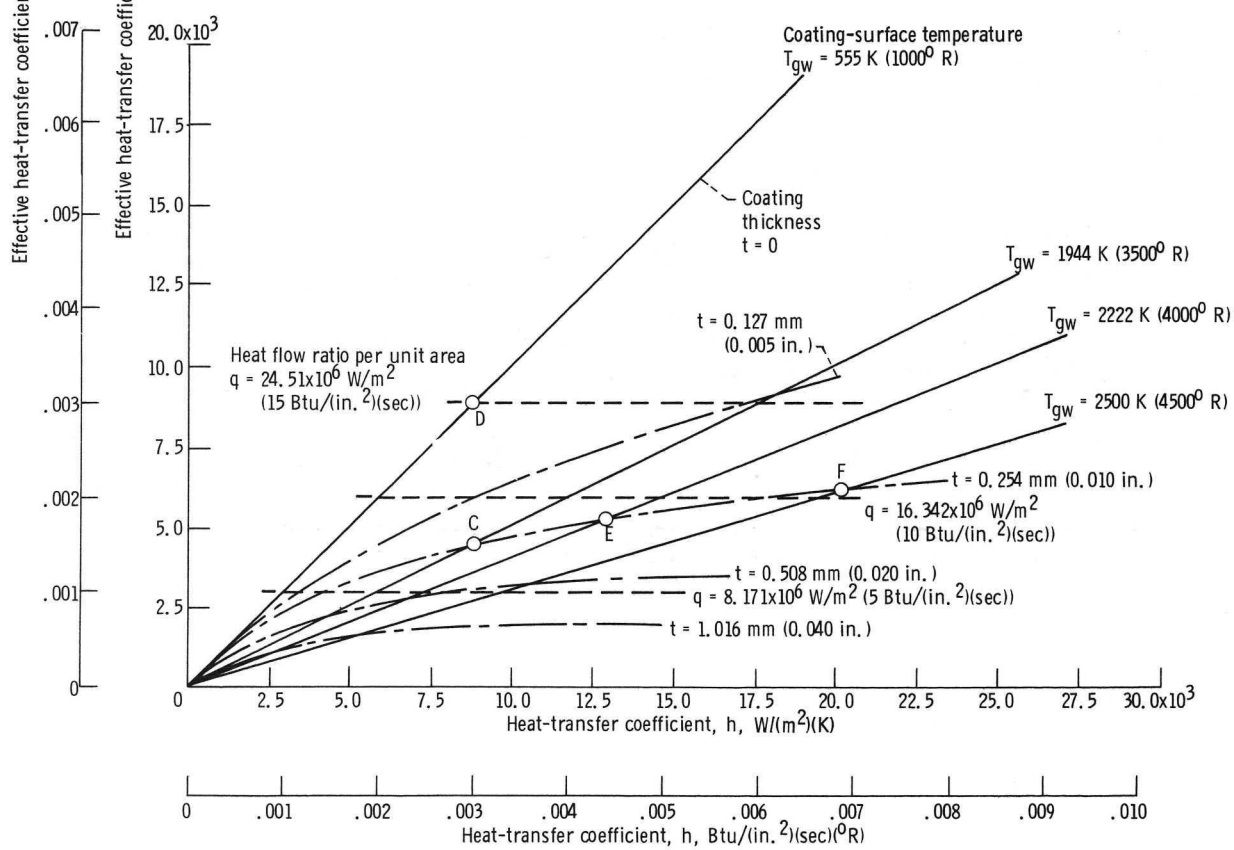

(b) Temperature of interface between wall metal and coating, T_{uw}, 555 K (1000° R).

Figure 8. - Coating thickness analysis. Thermal conductivity, k, 2.242 watts per meter kelvin (3x10^{-5} Btu/(in.)(sec)(°R)); adiabatic wall temperature, T_{aw}, 3333 K (6000° R).

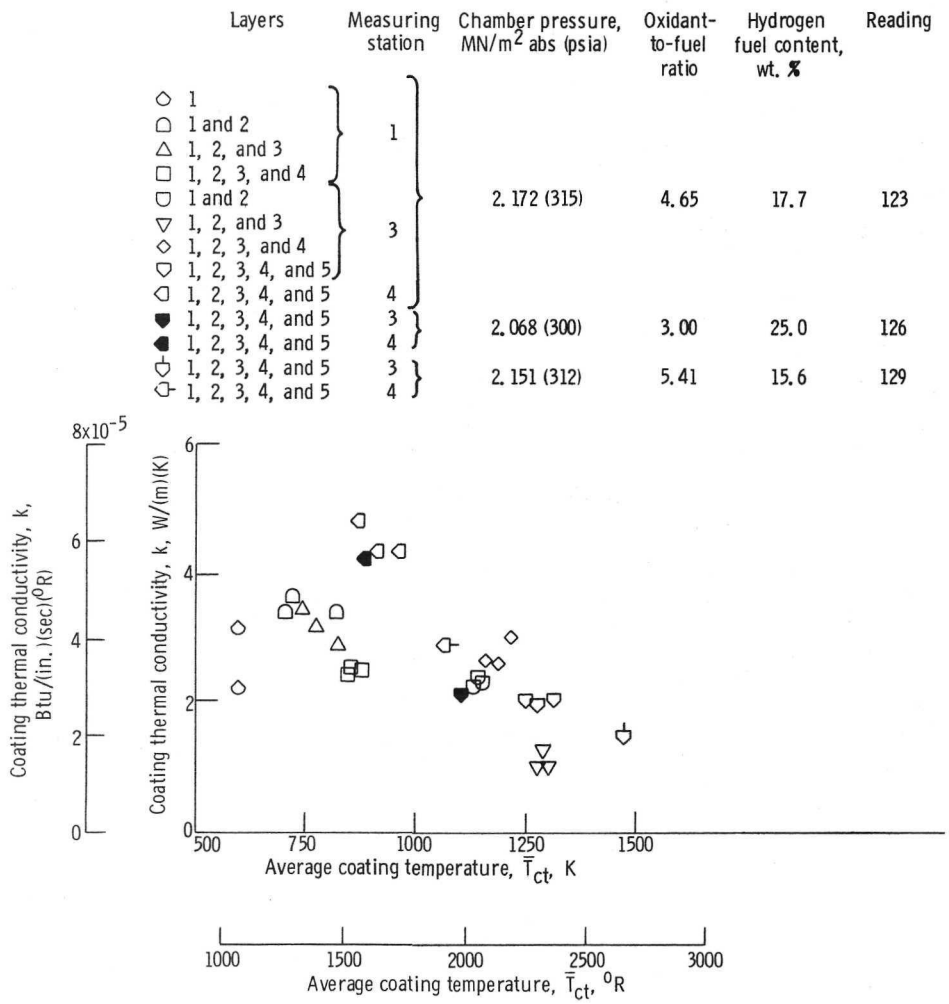

Figure 9. - Thermal conductivity as a function of average coating temperature for composite coating type 2 at all axial measuring stations in thrust chamber Cu II.

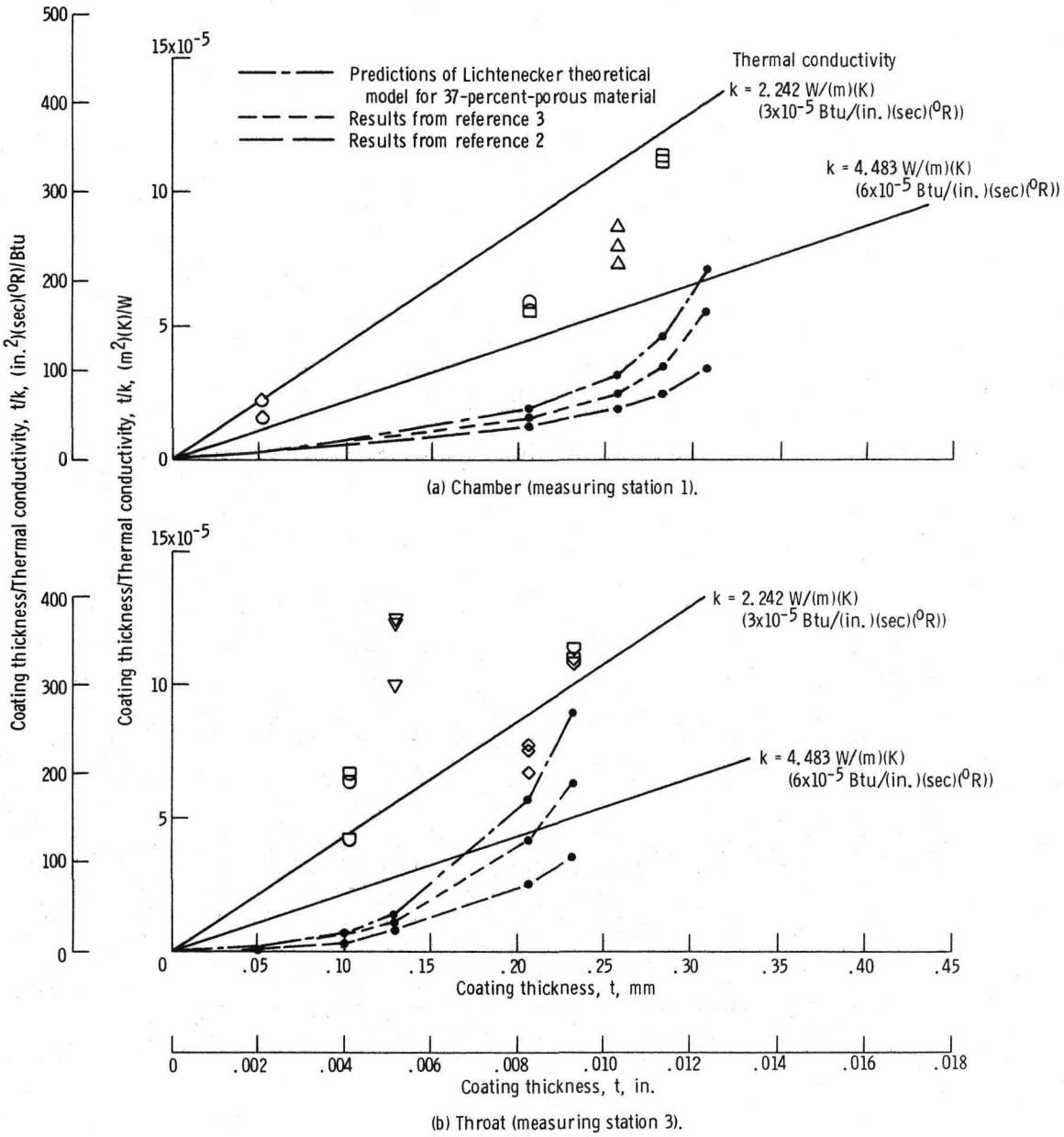

Figure 10. - Experimental conductivity compared with predictions of theoretical models for composite coating type 2.

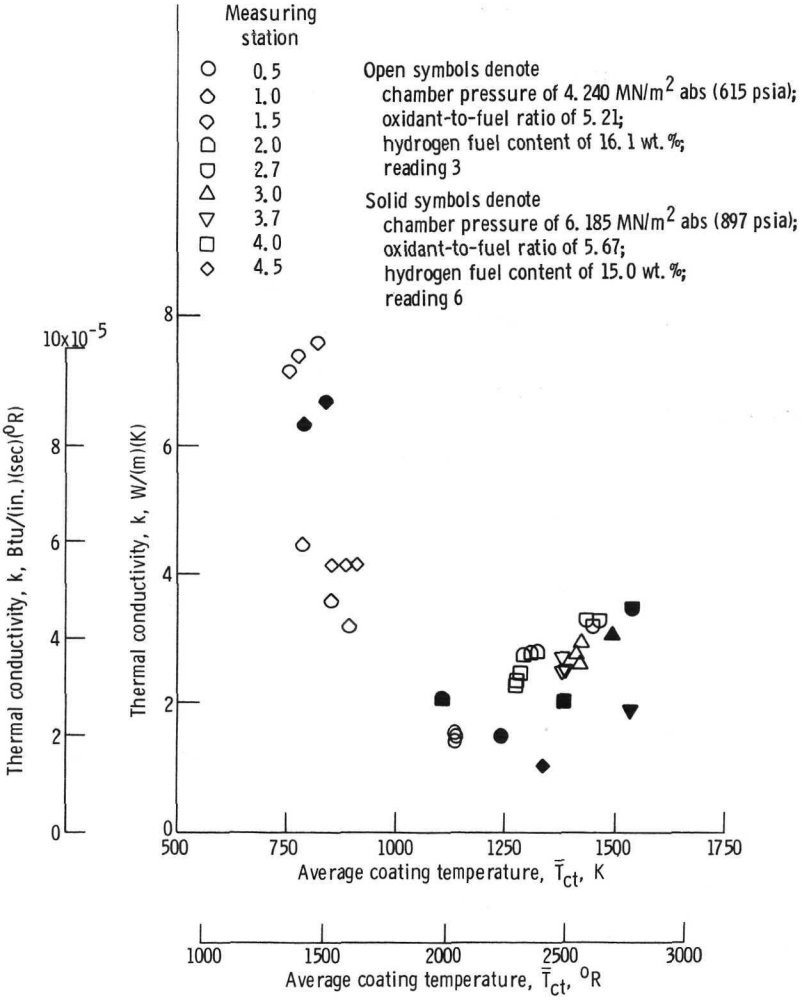

Figure 11. - Thermal conductivity as a function of average coating temperature for composite coating type 2 in thrust chamber Cu III.

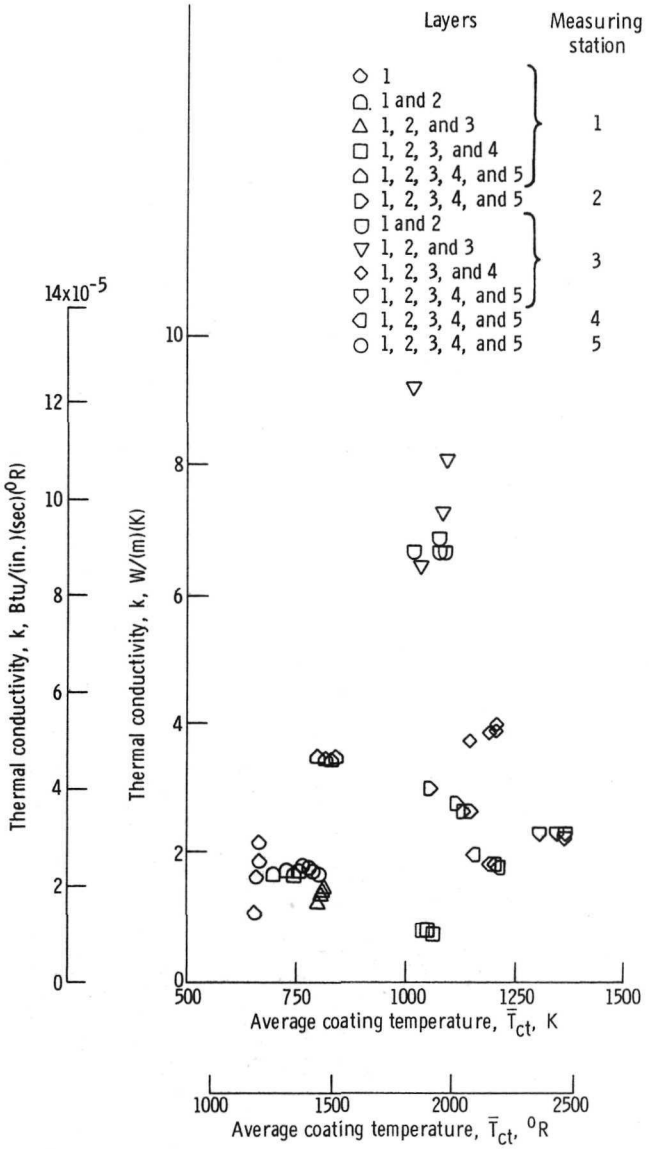

Figure 12. - Thermal conductivity as a function of average coating temperature for composite coating type 3 in thrust chamber Cu II. Chamber pressure, 2.068 meganewtons per square meter absolute (300 psia); oxidant-to-fuel ratio, 5.41; hydrogen fuel content, 15.6 weight percent.

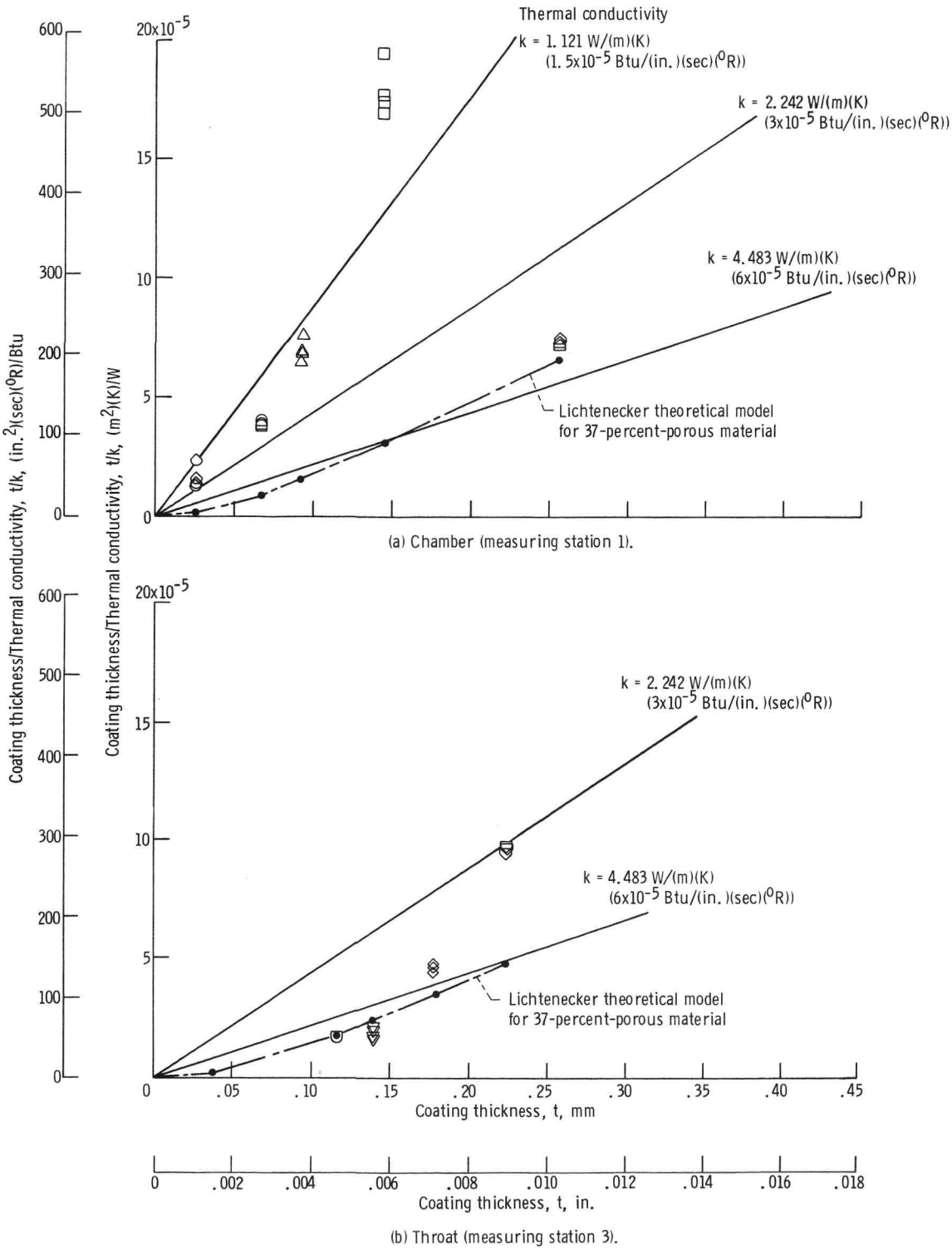

Figure 13. - Experimental conductivity of composite coating type 3 compared with predictions of theoretical model.

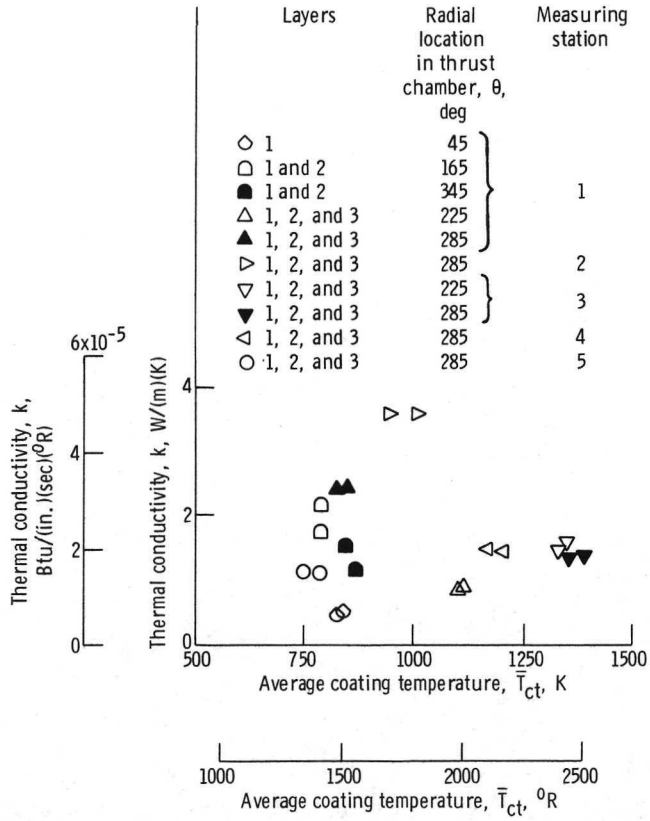

Figure 14. - Thermal conductivity as a function of average coating temperature for layered coating type 5 in thrust chamber Cu II. Chamber pressure, 2.068 meganewtons per square meter absolute (300 psia); oxidant-to-fuel ratio, 5.72; hydrogen fuel content, 14.9 weight percent; reading 177.

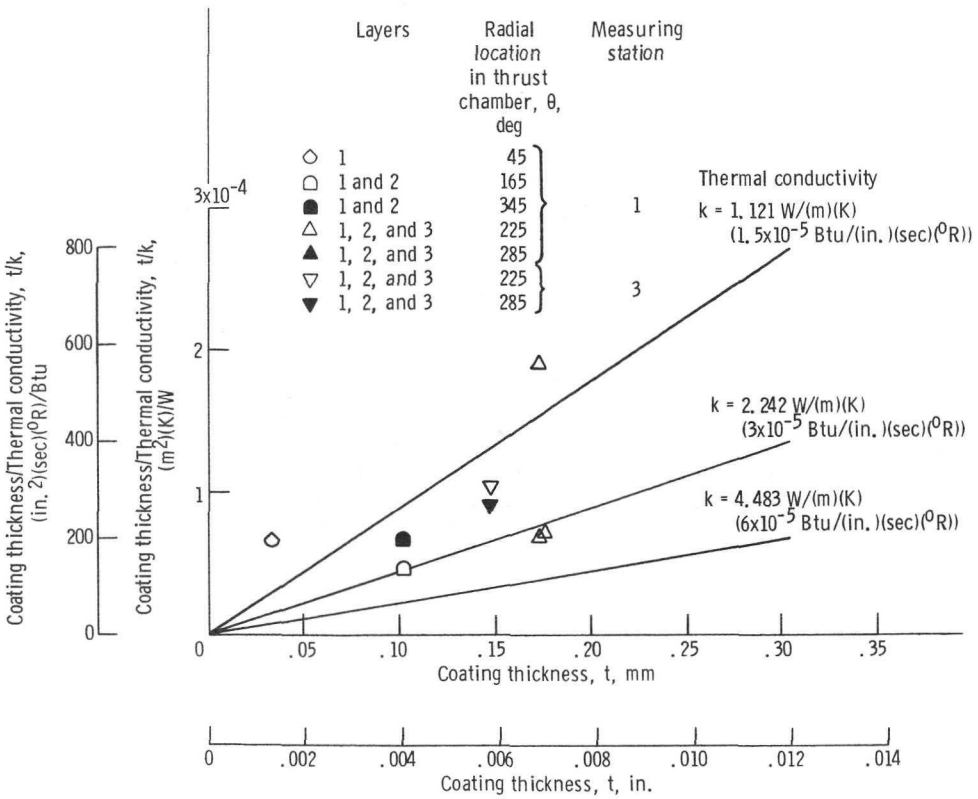

Figure 15. - Experimental conductivity compared with predictions of theoretical model for layered coating type 5. Reading 177.

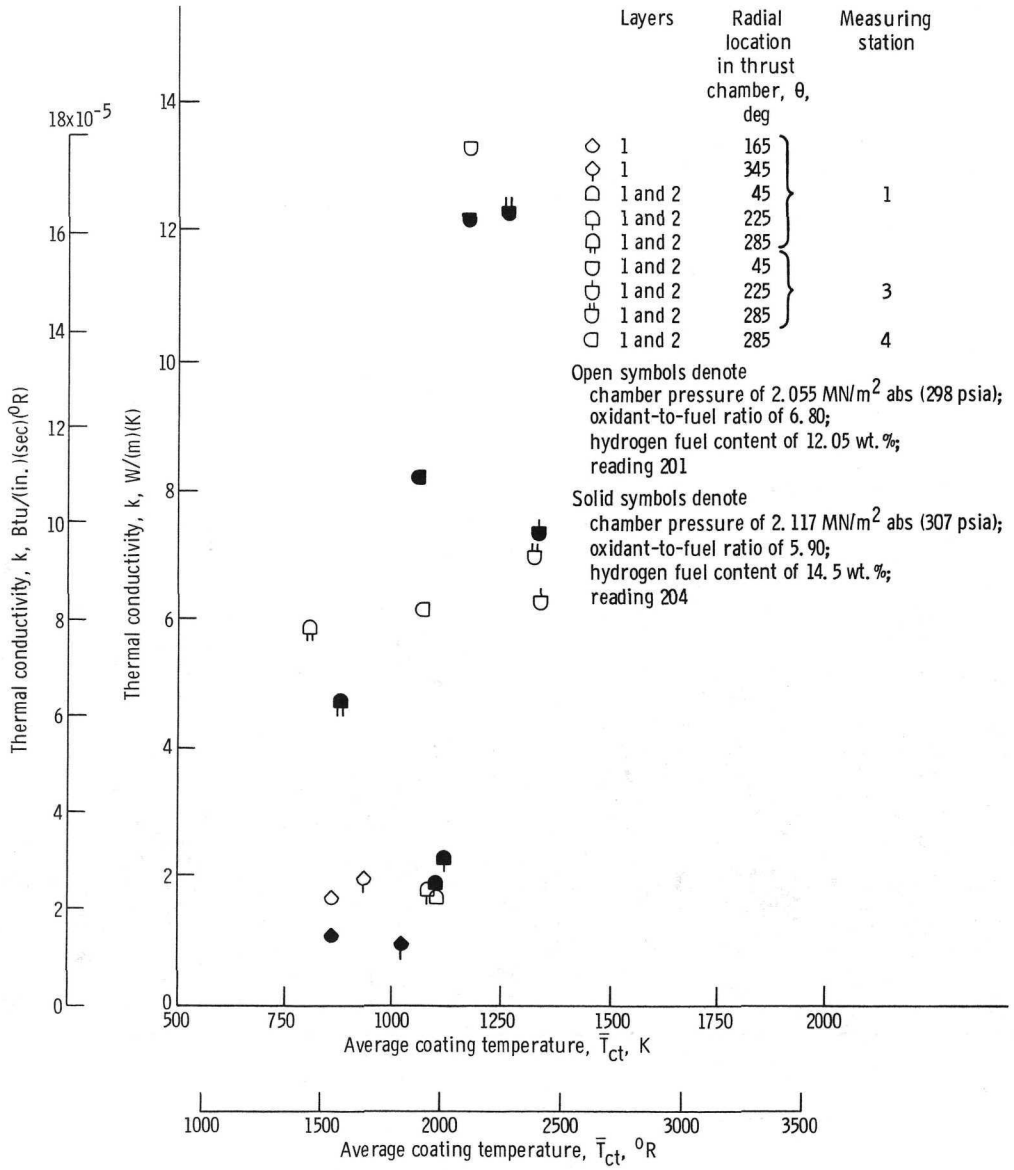

Figure 16. - Thermal conductivity as a function of average coating temperature for composite coating type 6 in thrust chamber Cu II.

NATIONAL AERONAUTICS AND SPACE ADMINISTRATION
WASHINGTON, D.C. 20546

OFFICIAL BUSINESS
PENALTY FOR PRIVATE USE $300

SPECIAL FOURTH-CLASS RATE
BOOK

POSTAGE AND FEES PAID
NATIONAL AERONAUTICS AND
SPACE ADMINISTRATION
451

U.S.MAIL

POSTMASTER : If Undeliverable (Section 158 Postal Manual) Do Not Return

"The aeronautical and space activities of the United States shall be conducted so as to contribute . . . to the expansion of human knowledge of phenomena in the atmosphere and space. The Administration shall provide for the widest practicable and appropriate dissemination of information concerning its activities and the results thereof."

—NATIONAL AERONAUTICS AND SPACE ACT OF 1958

NASA SCIENTIFIC AND TECHNICAL PUBLICATIONS

TECHNICAL REPORTS: Scientific and technical information considered important, complete, and a lasting contribution to existing knowledge.

TECHNICAL NOTES: Information less broad in scope but nevertheless of importance as a contribution to existing knowledge.

TECHNICAL MEMORANDUMS: Information receiving limited distribution because of preliminary data, security classification, or other reasons. Also includes conference proceedings with either limited or unlimited distribution.

CONTRACTOR REPORTS: Scientific and technical information generated under a NASA contract or grant and considered an important contribution to existing knowledge.

TECHNICAL TRANSLATIONS: Information published in a foreign language considered to merit NASA distribution in English.

SPECIAL PUBLICATIONS: Information derived from or of value to NASA activities. Publications include final reports of major projects, monographs, data compilations, handbooks, sourcebooks, and special bibliographies.

TECHNOLOGY UTILIZATION PUBLICATIONS: Information on technology used by NASA that may be of particular interest in commercial and other non-aerospace applications. Publications include Tech Briefs, Technology Utilization Reports and Technology Surveys.

Details on the availability of these publications may be obtained from:

SCIENTIFIC AND TECHNICAL INFORMATION OFFICE

NATIONAL AERONAUTICS AND SPACE ADMINISTRATION

Washington, D.C. 20546